cost of preserving the cold chain for currently used vaccines has been estimated at approximately US$300 million a year [88]. In addition, inappropriate disposal of needles and syringes poses a threat of environmental contamination and increases the risk of secondhand use, which can lead to the spread of secondary infectious diseases [88]. Thus, we must develop mucosal vaccines, which do not require dangerous administration devices or a cold chain, to combat emerging and re-emerging infectious diseases while addressing issues of cost, safety and the environment.

Five-year view

Because mucosal administration of vaccines can induce both systemic and mucosal immune responses, mucosal vaccination might improve the efficacy of current parentally delivered vaccines and provide a basis for preventing a range of infectious diseases that are initiated at the mucosal surfaces of the digestive, respiratory and reproductive tracts. However, some inactivated or subunit-type vaccines, which offer attractive safety profiles, are generally poor immunogens when given mucosally [6]. Thus, we propose a system of delivery of vaccine antigen to M cells. The development of M-cell-targeting systems for antigen delivery could increase the efficacy of mucosal vaccines for the induction of antigen-specific systemic and mucosal immune responses. To this end, we believe that the MucoRice system is an attractive and promising strategy for vaccination without the need for needles, syringes, or a cold chain [100], and the development of an M cell-targeted MucoRice vaccine may be the most promising approach to create an effective mucosal vaccine.

Financial & competing interests disclosure

The work was supported by the grants from Bill & Melinda Gates Foundation *in US, Scientific Research Priority Areas and Global Center Excellence from* the Ministry of Education, Culture, Sports, Science and Technology of Japan, the Ministry of Health and Labor of Japan, the Ministry of Economy, Trade and Industry of Japan (Hong Kong) and Bio-oriented Technology Research Advancement Institution in Japan (Saitama). The authors have no other *relevant affiliations or financial involvement with any organization or entity with a financial interest in or financial conflict with the subject matter or* materials discussed in the manuscript apart from those disclosed.

No writing assistance was utilized in the production of this manuscript.

Key issues

- Other than FluMist™, no nasal vaccines are currently available against most bacterial respiratory pathogens, including Streptococcus *pneumonia, Haemophilus influenza, Mycobacterium* tuberculosis and Bordetella pertussis.
- Transcutaneous and sublingual vaccines are nonclassical mucosal vaccines that can effectively induce both mucosal and systemic immunity for the prevention of infectious diseases.
- Creation of a novel mucosal-targeting system, such as M cell- and/or mucosal dendritic cell-targeted vaccine delivery, is a key issue for the development of effective mucosal vaccines.
- Mucosal adjuvants must also be developed for the induction of effective protective immunity against emerging and reemerging infectious diseases.
- Cold chain-free and needle/syringe-free vaccines are needed, especially in developing countries. A rice-based vaccine, MucoRice™, is currently one of the best candidates for achieving this goal.
- Registered mucosal vaccines are still few in number. Public-health requires effective and safe mucosal vaccines to control both emerging and re-emerging infectious diseases.

References

Papers of special note have been highlighted as:
• of interest
•• of considerable interest

1 Yuki Y, Nochi T, Kiyono H. Progress towards an AIDS mucosal vaccine: an overview. Tuberculosis (Edinb.) 87(Suppl. 1), S35–S44 (2007).

2 Holmgren J, Czerkinsky C. Mucosal immunity and vaccines. Nat. Med. 11(4 Suppl.), S45–S53 (2005).

• **Excellent review of mucosal vaccine and mucosal immunity.**

3 Quiding M, Nordstrom I, Kilander A et al. Intestinal immune responses in humans. Oral cholera vaccination induces strong intestinal antibody responses and interferon-γ production and evokes local immunological memory. J. Clin. Invest. 88(1), 143–148 (1991).

4 Johansson EL, Wassen L, Holmgren J, Jertborn M, Rudin A. Nasal and vaginal vaccinations have differential effects on antibody responses in vaginal and cervical secretions in humans. Infect. Immun. 69(12), 7481–7486 (2001).

5 Czerkinsky C, Anjuere F, McGhee JR et al. Mucosal immunity and tolerance: relevance to vaccine development. Immunol. Rev. 170, 197–222 (1999).

6 Mestecky J, Russell MW, Elson CO. Perspectives on mucosal vaccines: is mucosal tolerance a barrier? J. Immunol. 179(9), 5633–5638 (2007).

7 Yuki Y, Kiyono H. New generation of mucosal adjuvants for the induction of protective immunity. Rev. Med. Virol. 13(5), 293–310 (2003).

8 Kunisawa J, Kiyono H. A marvel of mucosal T cells and secretory antibodies for the creation of first lines of defense. Cell Mol. Life Sci. 62(12), 1308–1321 (2005).

9 Kiyono H, Fukuyama S. NALT- versus Peyer's-patch-mediated mucosal immunity. Nat. Rev. Immunol. 4(9), 699–710 (2004).

10 Neutra MR, Kozlowski PA. Mucosal vaccines: the promise and the challenge. Nat. Rev. Immunol. 6(2), 148–158 (2006).

11 Muramatsu M, Kinoshita K, Fagarasan S, Yamada S, Shinkai Y, Honjo T. Class switch recombination and hypermutation require activation-induced cytidine deaminase (AID), a potential RNA editing enzyme. Cell 102(5), 553–563 (2000).

12 Stagg AJ, Kamm MA, Knight SC. Intestinal dendritic cells increase T cell expression of α4β7 integrin. Eur. J. Immunol. 32(5), 1445–1454 (2002).

13 Johansson-Lindbom B, Svensson M, Wurbel MA, Malissen B, Marquez G, Agace W. Selective generation of gut tropic T cells in gut-associated lymphoid tissue (GALT): requirement for GALT dendritic cells and adjuvant. J. Exp. Med. 198(6), 963–969 (2003).

14 Mora JR, Bono MR, Manjunath N et al. Selective imprinting of gut-homing T cells by Peyer's patch dendritic cells. Nature 424(6944), 88–93 (2003).

15 Iwata M, Hirakiyama A, Eshima Y, Kagechika H, Kato C, Song SY. Retinoic acid imprints gut-homing specificity on T cells. Immunity 21(4), 527–538 (2004).

16 Mora JR, Iwata M, Eksteen B et al. Generation of gut-homing IgA-secreting B cells by intestinal dendritic cells. Science 314(5802), 1157–1160 (2006).

17 Campbell JJ, Brightling CE, Symon FA et al. Expression of chemokine receptors by lung T cells from normal and asthmatic subjects. J. Immunol. 166(4), 2842–2848 (2001).

18 Kunisawa J, Fukuyama S, Kiyono H. Mucosa-associated lymphoid tissues in the aerodigestive tract: their shared and divergent traits and their importance to the orchestration of the mucosal immune system. Curr. Mol. Med. 5(6), 557–572 (2005).

19 McGhee JR, Fujihashi K, Beagley KW, Kiyono H. Role of interleukin-6 in human and mouse mucosal IgA plasma cell responses. Immunol. Res. 10(3–4), 418–422 (1991).

20 Kaetzel CS. The polymeric immunoglobulin receptor: bridging innate and adaptive immune responses at mucosal surfaces. Immunol. Rev. 206, 83–99 (2005).

21 Brandtzaeg P, Prydz H. Direct evidence for an integrated function of J chain and secretory component in epithelial transport of immunoglobulins. Nature 311(5981), 71–73 (1984).

22 Neutra MR, Frey A, Kraehenbuhl JP. Epithelial M cells: gateways for mucosal infection and immunization. Cell 86(3), 345–348 (1996).

23 Iwasaki A. Mucosal dendritic cells. Annu. Rev. Immunol. 25, 381–418 (2007).

24 Rescigno M, Urbano M, Valzasina B et al. Dendritic cells express tight junction proteins and penetrate gut epithelial monolayers to sample bacteria. Nat. Immunol. 2(4), 361–367 (2001).

25 Jang MH, Kweon MN, Iwatani K et al. Intestinal villous M cells: an antigen entry site in the mucosal epithelium. Proc. Natl Acad. Sci. USA 101(16), 6110–6115 (2004).

26 Romani N, Ratzinger G, Pfaller K et al. Migration of dendritic cells into lymphatics – the Langerhans cell example: routes, regulation, and relevance. Int. Rev. Cytol. 207, 237–270 (2001).

27 Glenn GM, Rao M, Matyas GR, Alving CR. Skin immunization made possible by cholera toxin. Nature 391(6670), 851 (1998).

28 Cuburu N, Kweon MN, Song JH et al. Sublingual immunization induces broad-based systemic and mucosal immune responses in mice. Vaccine 25(51), 8598–8610 (2007).

29 Girard MP, Steele D, Chaignat CL, Kieny MP. A review of vaccine research and development: human enteric infections. Vaccine 24(15), 2732–2750 (2006).

30 Chumakov K, Ehrenfeld E, Wimmer E, Agol VI. Vaccination against polio should not be stopped. Nat. Rev. Microbiol. 5(12), 952–958 (2007).

31 He Y, Mueller S, Chipman PR et al. Complexes of poliovirus serotypes with their common cellular receptor, CD155. J. Virol. 77(8), 4827–4835 (2003).

32 Prevots DR, Sutter RW, Strebel PM, Weibel RE, Cochi SL. Completeness of reporting for paralytic poliomyelitis, United States, 1980 through 1991. Implications for estimating the risk of vaccine-associated disease. Arch. Pediatr. Adolesc. Med. 148(5), 479–485 (1994).

33 Kew O, Morris-Glasgow V, Landaverde M et al. Outbreak of poliomyelitis in Hispaniola associated with circulating type 1 vaccine-derived poliovirus. Science 296(5566), 356–359 (2002).

• **Report regarding vaccine-derived poliomyelitis.**

34 Sack DA, Sack RB, Nair GB, Siddique AK. Cholera. Lancet 363(9404), 223–233 (2004).

35 Levine MM, Kaper JB. Live oral vaccines against cholera: an update. Vaccine 11(2), 207–212 (1993).

36 Su-Arehawaratana P, Singharaj P, Taylor DN et al. Safety and immunogenicity of different immunization regimens of CVD 103-HgR live oral cholera vaccine in soldiers and civilians in Thailand. J. Infect. Dis. 165(6), 1042–1048 (1992).

37 Richie EE, Punjabi NH, Sidharta YY et al. Efficacy trial of single-dose live oral cholera vaccine CVD 103-HgR in North Jakarta, Indonesia, a cholera-endemic area. Vaccine 18(22), 2399–2410 (2000).

38 Clemens JD, Sack DA, Harris JR et al. Field trial of oral cholera vaccines in Bangladesh: results from three-year follow-up. Lancet 335(8684), 270–273 (1990).

39 Clemens JD, Sack DA, Harris JR et al. Impact of B subunit killed whole-cell and killed whole-cell-only oral vaccines against cholera upon treated diarrhoeal illness and mortality in an area endemic for cholera. Lancet 1(8599), 1375–1379 (1988).

40 Clemens JD, Sack DA, Harris JR et al. Field trial of oral cholera vaccines in Bangladesh. Lancet 2(8499), 124–127 (1986).

41 Ali M, Emch M, von Seidlein L et al. Herd immunity conferred by killed oral cholera vaccines in Bangladesh: a reanalysis. Lancet 366(9479), 44–49 (2005).

42 Lucas ME, Deen JL, von Seidlein L et al. Effectiveness of mass oral cholera vaccination in Beira, Mozambique. N. Engl. J. Med. 352(8), 757–767 (2005).

43 Clemens JD, Sack DA, Harris JR et al. Cross-protection by B subunit-whole cell cholera vaccine against diarrhea associated with heat-labile toxin-producing enterotoxigenic Escherichia coli: results of a large-scale field trial. J. Infect. Dis. 158(2), 372–377 (1988).

44 Kenner JR, Coster TS, Taylor DN et al. Peru-15, an improved live attenuated oral vaccine candidate for Vibrio cholerae O1. J. Infect. Dis. 172(4), 1126–1129 (1995).

45 Qadri F, Chowdhury MI, Faruque SM et al. Randomized, controlled study of the safety and immunogenicity of Peru-15, a live attenuated oral vaccine candidate for cholera, in adult volunteers in Bangladesh. J. Infect. Dis. 192(4), 573–579 (2005).

46 Qadri F, Chowdhury MI, Faruque SM et al. Peru-15, a live attenuated oral cholera Vaccine is safe and immunogenic in Bangladeshi toddlers and infants. Vaccine 25(2), 231–238 (2007).

47 Garmory HS, Brown KA, Titball RW. Salmonella vaccines for use in humans: present and future perspectives. FEMS Microbiol. Rev. 26(4), 339–353 (2002).

48 Sinha A, Sazawal S, Kumar R et al. Typhoid fever in children aged less than 5 years. Lancet 354(9180), 734–737 (1999).

49 Klugman KP, Koornhof HJ, Robbins JB, Le Cam NN. Immunogenicity, efficacy and serological correlate of protection of Salmonella typhi Vi capsular polysaccharide vaccine three years after immunization. Vaccine 14(5), 435–438 (1996).

50 Kossaczka Z, Lin FY, Ho VA et al. Safety and immunogenicity of Vi conjugate vaccines for typhoid fever in adults, teenagers, and 2- to 4-year-old children in Vietnam. Infect. Immun. 67(11), 5806–5810 (1999).

51 Gentschev I, Spreng S, Sieber H et al. Vivotif – a 'magic shield' for protection against typhoid fever and delivery of heterologous antigens. Chemotherapy, 53(3), 177–180 (2007).

52 Levine MM, Ferreccio C, Abrego P, Martin OS, Ortiz E, Cryz S. Duration of efficacy of Ty21a, attenuated Salmonella typhi live oral vaccine. Vaccine 17 Suppl 2, S22–27 (1999).

53 Dietrich G, Griot-Wenk M, Metcalfe IC, Lang AB, Viret JF. Experience with registered mucosal vaccines. Vaccine 21(7–8), 678–683 (2003).

54 Salerno-Goncalves R, Pasetti MF, Sztein MB. Characterization of CD8+ effector T cell responses in volunteers immunized with Salmonella enterica serovar Typhi strain Ty21a typhoid vaccine. J. Immunol. 169(4), 2196–2203 (2002).

55 Nakagomi O, Cunliffe NA. Rotavirus vaccines: entering a new stage of deployment. Curr. Opin. Infect. Dis. 20(5), 501–507 (2007).

56 DiPetrillo MD, Tibbetts T, Kleanthous H, Killeen KP, Hohmann EL. Safety and immunogenicity of phoP/phoQ-deleted Salmonella typhi expressing Helicobacter pylori urease in adult volunteers. Vaccine 18(5–6), 449–459 (1999).

57 Witherell GW. Oral typhoid vaccine. Acambis/Berna. Curr. Opin. Investig. Drugs 4(8), 1010–1018 (2003).

58 Parashar UD, Hummelman EG, Bresee JS, Miller MA, Glass RI. Global illness and deaths caused by rotavirus disease in children. Emerg. Infect. Dis. 9(5), 565–572 (2003).

59 Santos N, Hoshino Y. Global distribution of rotavirus serotypes/genotypes and its implication for the development and implementation of an effective rotavirus vaccine. Rev. Med. Virol. 15(1), 29–56 (2005).

60 Bines JE. Intussusception and rotavirus vaccines. Vaccine 24(18), 3772–3776 (2006).

61 Simonsen L, Morens D, Elixhauser A, Gerber M, Van Raden M, Blackwelder W. Effect of rotavirus vaccination programme on trends in admission of infants to hospital for intussusception. Lancet 358(9289), 1224–1229 (2001).

62 Bernstein DI, Sack DA, Rothstein E et al. Efficacy of live, attenuated, human rotavirus vaccine 89–12 in infants: a randomised placebo-controlled trial. Lancet 354(9175), 287–290 (1999).

63 Ruiz-Palacios GM, Perez-Schael I, Velazquez FR et al. Safety and efficacy of an attenuated vaccine against severe rotavirus gastroenteritis. N. Engl. J. Med. 354(1), 11–22 (2006).

64 Vesikari T, Matson DO, Dennehy P et al. Safety and efficacy of a pentavalent human-bovine (WC3) reassortant rotavirus vaccine. N. Engl. J. Med. 354(1), 23–33 (2006).

65 Franco MA, Angel J, Greenberg HB. Immunity and correlates of protection for rotavirus vaccines. Vaccine 24(15), 2718–2731 (2006).

66 Michaud CM, Murray CJ, Bloom BR. Burden of disease – implications for future research. JAMA 285(5), 535–539 (2001).

67 Girard MP, Cherian T, Pervikov Y, Kieny MP. A review of vaccine research and development: human acute respiratory infections. Vaccine 23(50), 5708–5724 (2005).

68 Izurieta HS, Thompson WW, Kramarz P et al. Influenza and the rates of hospitalization for respiratory disease among infants and young children. N. Engl. J. Med. 342(4), 232–239 (2000).

69 Cox RJ, Brokstad KA, Ogra P. Influenza virus: immunity and vaccination strategies. Comparison of the immune response to inactivated and live, attenuated influenza vaccines. Scand. J. Immunol. 59(1), 1–15 (2004).

70 Belshe RB. Current status of live attenuated influenza virus vaccine in the US. Virus Res. 103(1–2), 177–185 (2004).

71 Youngner JS, Treanor JJ, Betts RF, Whitaker-Dowling P. Effect of simultaneous administration of cold-adapted and wild-type influenza A viruses on experimental wild-type influenza infection in humans. J. Clin. Microbiol. 32(3), 750–754 (1994).

72 Maassab HF. Adaptation and growth characteristics of influenza virus at 25 degrees C. Nature 213(5076), 612–614 (1967).

•• **Original paper of cold-adapted influenza virus that is used as the first nasal influenza vaccine.**

73 Belshe RB, Edwards KM, Vesikari T et al. Live attenuated versus inactivated influenza vaccine in infants and young children. N. Engl. J. Med. 356(7), 685–696 (2007).

74 Durbin AP, Karron RA. Progress in the development of respiratory syncytial virus and parainfluenza virus vaccines. Clin. Infect. Dis. 37(12), 1668–1677 (2003).

75 Tang RS, MacPhail M, Schickli JH et al. Parainfluenza virus type 3 expressing the native or soluble fusion (F) protein of respiratory syncytial virus (RSV) confers protection from RSV infection in African green monkeys. J. Virol. 78(20), 11198–11207 (2004).

76 Flynn JL, Chan J. Immunology of tuberculosis. Annu. Rev. Immunol. 19, 93–129 (2001).

77 Skeiky YA, Sadoff JC. Advances in tuberculosis vaccine strategies. Nat. Rev. Microbiol. 4(6), 469–476 (2006).

78 Baumann U. Mucosal vaccination against bacterial respiratory infections. Expert Rev. Vaccines 7(8), 1257–1276 (2008).

79 McShane H, Pathan AA, Sander CR, Goonetilleke NP, Fletcher HA, Hill AV. Boosting BCG with MVA85A: the first candidate subunit vaccine for tuberculosis in clinical trials. Tuberculosis (Edinb.) 85(1–2), 47–52 (2005).

80 Santosuosso M, McCormick S, Zhang X, Zganiacz A, Xing Z. Intranasal boosting with an adenovirus-vectored vaccine markedly enhances protection by parenteral Mycobacterium bovis BCG immunization against pulmonary tuberculosis. Infect. Immun. 74(8), 4634–4643 (2006).

81 Brandt L, Oettinger T, Holm A, Andersen AB, Andersen P. Key epitopes on the ESAT-6 antigen recognized in mice during the recall of protective immunity to Mycobacterium tuberculosis. J. Immunol. 157(8), 3527–3533 (1996).

82 Lycke N. From toxin to adjuvant: the rational design of a vaccine adjuvant vector, CTA1-DD/ISCOM. Cell Microbiol. 6(1), 23–32 (2004).

83 Mowat AM, Donachie AM, Jagewall S et al. CTA1-DD-immune stimulating complexes: a novel, rationally designed combined mucosal vaccine adjuvant effective with nanogram doses of antigen. J. Immunol. 167(6), 3398–3405 (2001).

84 Andersen CS, Dietrich J, Agger EM, Lycke NY, Lovgren K, Andersen P. The combined CTA1-DD/ISCOMs vector is an effective intranasal adjuvant for boosting prior Mycobacterium bovis BCG immunity to Mycobacterium tuberculosis. Infect. Immun. 75(1), 408–416 (2007).

85 Eriksson AM, Schon KM, Lycke NY. The cholera toxin-derived CTA1-DD vaccine adjuvant administered intranasally does not cause inflammation or accumulate in the nervous tissues. J. Immunol. 173(5), 3310–3319 (2004).

86 Goonetilleke NP, McShane H, Hannan CM, Anderson RJ, Brookes RH, Hill AV. Enhanced immunogenicity and protective efficacy against Mycobacterium tuberculosis of bacille Calmette–Guerin vaccine using mucosal administration and boosting with a recombinant modified vaccinia virus Ankara. J. Immunol. 171(3), 1602–1609 (2003).

87 McShane H, Pathan AA, Sander CR et al. Recombinant modified vaccinia virus Ankara expressing antigen 85A boosts BCG-primed and naturally acquired antimycobacterial immunity in humans. Nat. Med. 10(11), 1240–1244 (2004).

88 Giudice EL, Campbell JD. Needle-free vaccine delivery. Adv. Drug Deliv. Rev. 58(1), 68–89 (2006).

89 Glenn GM, Taylor DN, Li X, Frankel S, Montemarano A, Alving CR. Transcutaneous immunization: a human vaccine delivery strategy using a patch. Nat. Med. 6(12), 1403–1406 (2000).

90 Belyakov IM, Hammond SA, Ahlers JD, Glenn GM, Berzofsky JA. Transcutaneous immunization induces mucosal CTLs and protective immunity by migration of primed skin dendritic cells. J. Clin. Invest. 113(7), 998–1007 (2004).

91 Chang SY, Cha HR, Igarashi O et al. Cutting edge: Langerin + dendritic cells in the mesenteric lymph node set the stage for skin and gut immune system cross-talk. J. Immunol. 180(7), 4361–4365 (2008).

92 Glenn GM, Villar CP, Flyer DC et al. Safety and immunogenicity of an enterotoxigenic Escherichia coli vaccine patch containing heat-labile toxin: use of skin pretreatment to disrupt the stratum corneum. Infect. Immun. 75(5), 2163–2170 (2007).

93 Steinsland H, Valentiner-Branth P, Gjessing HK, Aaby P, Molbak K, Sommerfelt H. Protection from natural infections with enterotoxigenic Escherichia coli: longitudinal study. Lancet 362(9380), 286–291 (2003).

94 Streatfield SJ, Howard JA. Plant-based vaccines. Int. J. Parasitol. 33(5–6), 479–493 (2003).

95 Ma JK, Drake PM, Christou P. The production of recombinant pharmaceutical proteins in plants. Nat. Rev. Genet. 4(10), 794–805 (2003).

96 Streatfield SJ. Mucosal immunization using recombinant plant-based oral vaccines. Methods 38(2), 150–157 (2006).

97 Haq TA, Mason HS, Clements JD, Arntzen CJ. Oral immunization with a recombinant bacterial antigen produced in transgenic plants. Science 268(5211), 714–716 (1995).

98 Tacket CO, Mason HS, Losonsky G, Estes MK, Levine MM, Arntzen CJ. Human immune responses to a novel norwalk virus vaccine delivered in transgenic potatoes. J. Infect. Dis. 182(1), 302–305 (2000).

99 Tacket CO, Pasetti MF, Edelman R, Howard JA, Streatfield S. Immunogenicity of recombinant LT-B delivered orally to humans in transgenic corn. Vaccine 22(31–32), 4385–4389 (2004).

100 Nochi T, Takagi H, Yuki Y et al. Rice-based mucosal vaccine as a global strategy for cold-chain- and needle-free vaccination. Proc. Natl Acad. Sci. USA 104(26), 10986–10991 (2007).

•• **First cold chain- and needle-free vaccine using rice-based delivery system.**

101 Brayden DJ, Jepson MA, Baird AW. Keynote review: intestinal Peyer's patch M cells and oral vaccine targeting. Drug Discov. Today 10(17), 1145–1157 (2005).

102 Sharma R, Schumacher U, Adam E. Lectin histochemistry reveals the appearance of M-cells in Peyer's patches of SCID mice after syngeneic normal bone marrow transplantation. J. Histochem. Cytochem. 46(2), 143–148 (1998).

103 Helander A, Silvey KJ, Mantis NJ et al. The viral sigma1 protein and glycoconjugates containing α2–3-linked sialic acid are involved in type 1 reovirus adherence to M cell apical surfaces. J. Virol. 77(14), 7964–7977 (2003).

104 Manocha M, Pal PC, Chitralekha KT et al. Enhanced mucosal and systemic immune response with intranasal immunization of mice with HIV peptides entrapped in PLG microparticles in combination with Ulex Europaeus-I lectin as M cell target. Vaccine 23(48–49), 5599–5617 (2005).

105 Wu Y, Wang X, Csencsits KL, Haddad A, Walters N, Pascual DW. M cell-targeted DNA vaccination. Proc. Natl Acad. Sci. USA 98(16), 9318–9323 (2001).

106 Nochi T, Yuki Y, Matsumura A et al. A novel M cell-specific carbohydrate-targeted mucosal vaccine effectively induces antigen-specific immune responses. J. Exp. Med. 204(12), 2789–2796 (2007).

• **M-cell-targeted vaccine using the first M cell-specific monoclonal antibody.**

107 Agostinis F, Tellarini L, Canonica GW, Falagiani P, Passalacqua G. Safety of sublingual immunotherapy with a monomeric allergoid in very young children. Allergy, 60(1), 133 (2005).

108 Wilson DR, Lima MT, Durham SR. Sublingual immunotherapy for allergic rhinitis: systematic review and meta-analysis. Allergy, 60(1), 4–12 (2005).

109 Kweon MN, Yamamoto M, Watanabe F et al. A nontoxic chimeric enterotoxin adjuvant induces protective immunity in both mucosal and systemic compartments with reduced IgE antibodies. J. Infect. Dis. 186(9), 1261–1269 (2002).

110 Song JH, Nguyen HH, Cuburu N et al. Sublingual vaccination with influenza virus protects mice against lethal viral infection. Proc. Natl Acad. Sci. USA 105(5), 1644–1649 (2008).

• **One of the few experimental studies on sublingual vaccination.**

111 Mutsch M, Zhou W, Rhodes P et al. Use of the inactivated intranasal influenza vaccine and the risk of Bell's palsy in Switzerland. N. Engl. J. Med. 350(9), 896–903 (2004).

112 van Ginkel FW, Jackson RJ, Yuki Y, McGhee JR. Cutting edge: the mucosal adjuvant cholera toxin redirects vaccine proteins into olfactory tissues. J. Immunol. 165(9), 4778–4782 (2000).

113 Kaisho T, Akira S. Toll-like receptors as adjuvant receptors. Biochim. Biophys. Acta 1589(1), 1–13 (2002).

114 Varmus H, Klausner R, Zerhouni E, Acharya T, Daar AS, Singer PA. Public health. Grand Challenges in Global Health. Science 302(5644), 398–399 (2003).

Patent

201 Curtiss RI, Cardineau CA. Oral immunisation by transgenic plants. US patent 5686079 (1998).

•• **First application of a plant-based vaccine.**

Websites

301 WHO. Water sanitation and health (WSH). Water-related diseases www.who.int/water_sanitation_health/diseases/diarrhoea/en/

302 US FDA. Vaccines, blood & biologics: FluMist (intranasal influenza virus vaccine) questions and answers www.fda.gov/BiologicsBloodVaccines/Vaccines/QuestionsaboutVaccines/ucm080754.htm

303 WHO. Global tuberculosis control www.who.int/tb/publications/global_report/2009/en/index.html

Affiliations

- Yoshikazu Yuki
  Division of Mucosal Immunology, Department of Microbiology and Immunology, The Institute of Medical Science, The University of Tokyo, Tokyo 108-8639, Japan
  Tel.: +81 3 5449 5274
  Fax: +81 3 5449 5411
  yukiy@ims.u-tokyo.ac.jp
- Hiroshi Kiyono
  Division of Mucosal Immunology, Department of Microbiology and Immunology, The Institute of Medical Science, The University of Tokyo, 4-6-1 Shirokanedai, Minato-ku, Tokyo 108-8639, Japan
  Tel.: +81 3 5449 5270
  Fax: +81 3 5449 5411
  kiyono@ims.u-tokyo.ac.jp

Bioorganic & Medicinal Chemistry Letters 20 (2010) 1241–1246

Contents lists available at ScienceDirect

Bioorganic & Medicinal Chemistry Letters

journal homepage: www.elsevier.com/locate/bmcl

Synthesis and biological evaluation of novel allophenylnorstatine-based HIV-1 protease inhibitors incorporating high affinity P2-ligands

Arun K. Ghosh [a,*], Sandra Gemma [a], Elena Simoni [a], Abigail Baldridge [a], D. Eric Walters [b], Kazuhiko Ide [c], Yasushi Tojo [c], Yasuhiro Koh [c], Masayuki Amano [c], Hiroaki Mitsuya [c,d]

[a] Departments of Chemistry and Medicinal Chemistry, Purdue University, West Lafayette, IN 47907, United States
[b] Departments of Biochemistry and Molecular Biology, Rosalind Franklin University of Medicine and Science, North Chicago, IL 60064, United States
[c] Departments of Hematology and Infectious Diseases, Kumamoto University School of Medicine, Kumamoto 860-8556, Japan
[d] Experimental Retrovirology Section, HIV and AIDS Malignancy Branch, National Cancer Institute, Bethesda, MD 20892, United States

ARTICLE INFO

Article history:
Received 19 October 2009
Revised 20 November 2009
Accepted 23 November 2009
Available online 5 December 2009

Keywords:
HIV protease
Inhibitors
Darunavir
Allophenylnorstatine
Design
Synthesis

ABSTRACT

A series of stereochemically defined cyclic ethers as P2-ligands were incorporated in an allophenylnorstatine-based isostere to provide a new series of HIV-1 protease inhibitors. Inhibitors **3b** and **3c**, containing conformationally constrained cyclic ethers, displayed impressive enzymatic and antiviral properties and represent promising lead compounds for further optimization.

The introduction of protease inhibitors into highly active antiretroviral treatment (HAART) regimens with reverse transcriptase inhibitors represented a major breakthrough in AIDS chemotherapy.[1] This combination therapy has significantly increased life expectancy, and greatly improved the course of HIV management. Therapeutic inhibition of HIV-1 protease leads to morphologically immature and noninfectious viral particles.[2] However, under the selective pressure of chemotherapeutics, rapid adaptation of viral enzymes generates strains resistant to one or more antiviral agents.[3] As a consequence, a growing number of HIV/AIDS patients harbor multidrug-resistant HIV strains. There is ample evidence that such strains can be readily transmitted.[4] Therefore, one of the major current therapeutic objectives has been to develop novel protease inhibitors (PIs) with broad-spectrum activity against multidrug-resistant HIV-1 variants. In our continuing interest in developing concepts and strategies to combat drug-resistance, we have reported a series of novel PIs including Darunavir, TMC-126, GRL-06579, and GRL-02031.[5–8] These inhibitors have shown exceedingly potent enzyme inhibitory and antiviral activity as well as exceptional broad spectrum activity against highly cross-resistant mutants. Darunavir, which incorporates a (*R*)-(hydroxymethyl)-sulfonamide isostere and a stereochemically defined bis-tetrahydrofuran (bis-THF) as the P2-ligand, was initially approved for the treatment of patients with drug-resistant HIV and more recently, it has been approved for all HIV/AIDS patients including pediatrics[9] (Fig. 1).

Darunavir was designed based upon the 'backbone binding' concept developed in our laboratories. Darunavir-bound X-ray structure revealed extensive hydrogen bonding with the protease backbone throughout the enzyme active site.[10] The P2-bis-THF ligand is responsible for its superior drug-resistance properties. The bis-THF ligand has been documented as a privileged ligand for the S2-subsite. Incorporation of this ligand into other transition-state isosteres also resulted in significant potency enhancement.[11] Besides 3(*S*)-THF, and [3*a*S,5*S*,6*R*]-bis-THF, we have designed a number of other novel cyclic ether-based high affinity ligands. Incorporation of these ligands in (*R*)-(hydroxyethyl)-sulfonamide isosteres provided PIs with excellent potency and drug-resistance properties.[6–8] We then investigated the potential of these structure-based designed P2-ligands in a KNI-764-derived isostere designed by Mimoto and coworkers.[12] This PI incorporates an allophenylnorstatine isostere. Interestingly, KNI-764 has maintained good activity against HIV-1 clinical strains resistant to several FDA-approved PIs. The flexible *N*-(2-methyl benzyl) amide P2′-ligand may have been responsible for its activity against drug-resistant HIV-1 strains as the flexible chain allows better adaptability to mutations.[12,13] The bis-THF and other structure-based designed P2-ligands, make several critical

* Corresponding author. Tel.: +1 765 494 5323; fax: +1 765 496 1612.
E-mail address: akghosh@purdue.edu (A.K. Ghosh).

0960-894X/$ - see front matter © 2009 Elsevier Ltd. All rights reserved.
doi:10.1016/j.bmcl.2009.11.123

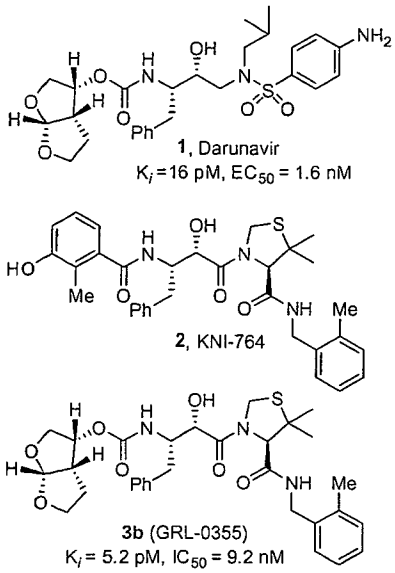

Figure 1. Structures of inhibitors **1**, **2**, and **3b**.

hydrogen bonds with the protein backbone, particularly with Asp-29 and Asp-30 NH's.[11] Therefore, incorporation of these ligands into the KNI-764-derived isostere, may lead to novel PIs with improved potency and efficacy against multidrug-resistant HIV-1 variants. Furthermore, substitution of the P2-phenolic derivative in KNI-764 with a cyclic ether-based ligand could result in improved metabolic stability and pharmacological properties since phenol glucuronide is readily formed when KNI-764 is exposed to human hepatocytes in vitro.[12]

The synthesis of target compounds **3a–e** was accomplished as described in Scheme 1. Our synthetic plan for carboxylic acid **7** (Scheme 1) involved the preparation of the key intermediate **5** through two different synthetic pathways. In the first approach, known optically active azidodiol **4**[14] was first hydrogenated in the presence of Boc_2O. The resulting diol was converted to **5** by selective acylation of the primary alcohol with acetic anhydride in the presence of pyridine and a catalytic amount of DMAP at 0 °C for 4 h to provide **5** in 77% overall yield. As an alternative approach, commercially available optically active epoxide **6** was exposed to lithium acetate, formed in situ from lithium carbonate and acetic acid in DMF. This resulted in the regioselective opening[15] of the epoxide ring and afforded compound **5** in 62% yield. The alcohol **5** thus obtained was protected as the corresponding acetonide by treatment with 2-methoxypropene in the presence of a catalytic amount of CSA. The acetate group was subsequently hydrolyzed in the presence of potassium carbonate in methanol to afford the corresponding alcohol. This was subjected to an oxidation reaction using ruthenium chloride hydrate and sodium periodate in a mixture of aqueous acetonitrile and CCl_4 at 23 °C for 10 h. This resulted in the formation of the target carboxylic acid **7** in 61% yield. Amide **9a** was prepared by activation of carboxylic acid **7** into the corresponding mixed anhydride by treatment with isobutylchloroformate followed by reaction with amine **8a**.[16,17]

Synthesis of various inhibitors was carried out as shown in Scheme 2. Deprotection of the Boc and acetonide groups was carried out by exposure of **9** to a 1 M solution of hydrochloric acid in methanol at 23 °C for 8 h. This provided amine **10** in quantitative

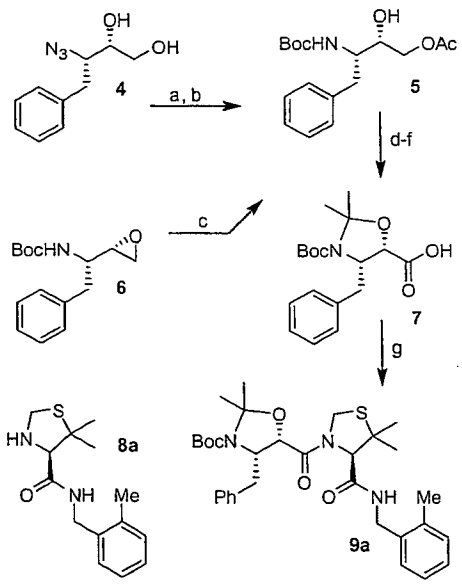

Scheme 1. Reagents: (a) H_2, Pd/C, Boc_2O, EtOAc; (b) Ac_2O, Pyr, DMAP; (c) $LiCO_3$, AcOH, DMF; (d) 2-methoxypropene, CSA, DCM; (e) K_2CO_3, MeOH; (f) $RuCl_3$, $NaIO_4$, CCl_4–MeCN–H_2O (2:2:3); (g) *N*-methylmorpholine, *i*BuOCOCl, **8a**, THF.

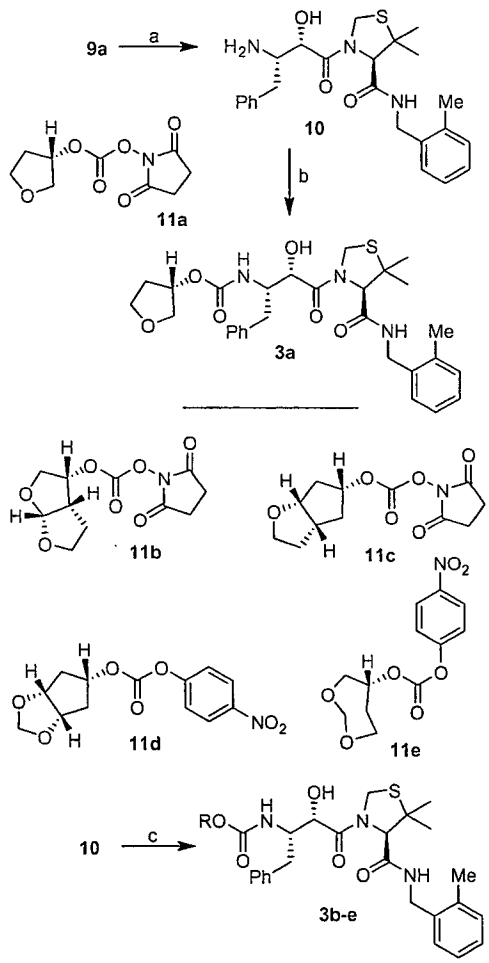

Scheme 2. Reagents: (a) 1 M HCl, MeOH; (b) **11a**, Et_3N, CH_2Cl_2; (c) **11b,c**, Et_3N, CH_2Cl_2; or, **11d,e**, DIPEA, THF.

yield. Reaction of **11a** with amine **10** in CH_2Cl_2 in the presence of Et_3N at 23 °C for 6 h, provided inhibitor **3a** in 62% yield. The 3(*S*)-tetrahydrofuranyl carbonate **11a** was prepared as described previously.[18] Similarly, allophenylnorstatine-based inhibitors **3b–e** were synthesized. As shown, carbonates **11b**,[19] **11c**,[7] and **11d–e**[19] were prepared as previously described. Reaction of these carbonates with amine **10** furnished the desired inhibitors **3b–e** in 45–62% yield.

The syntheses of inhibitors **14a,b** and **16a–c** were carried out as shown in Scheme 3. Inhibitors **14a,b**, containing hydroxyethylamine isostere were prepared by opening epoxide **6** with amine **8a** in the presence of lithium perchlorate in diethyl ether at 23 °C for 5 h to provide amino alcohol **12** in 64% yield. Removal of the Boc-group by exposure to 1 M HCl in MeOH at 23 °C for 12 h afforded amine **13**. Reactions of amine **13** with activated carbonates **11a** and **11b** afforded urethane **14a** and **14b** in 44% and 59% yields, respectively. For the synthesis of inhibitors **16a–c**, commercially available (*R*)-5,5-dimethyl-thiazolidine-4-carboxylic acid was protected as its Boc-derivative. The resulting acid was coupled with amines **15a–c** in the presence of DCC and DMAP in CH_2Cl_2 to provide the corresponding amides. Removal of the Boc-group by exposure to 30% trifluoroacetic acid afforded **8b–d**. Coupling of these amines with acid **7** as described in Scheme 1, provided the corresponding products **9b–d**. Removal of Boc-group and reactions of the resulting amines with activated carbonate **11b** furnished inhibitors **16a–c** in good yields (55–60%).

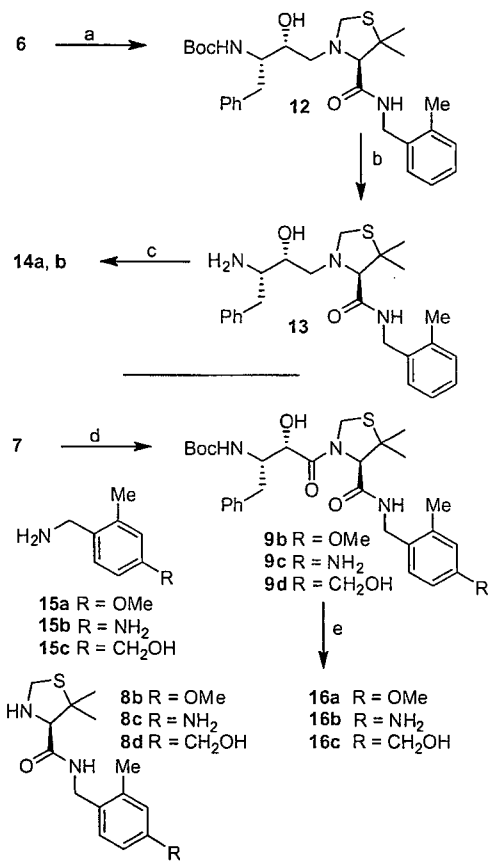

Scheme 3. Reagents: (a) **8a**, $Li(ClO_4)$, Et_2O; (b) CF_3CO_2H, CH_2Cl_2; (c) **11a** or, **11b**, Et_3N, CH_2Cl_2; (d) *N*-methylmorpholine, isobutylchloroformate, **8b-d**, THF; (e) CF_3CO_2H, CH_2Cl_2, then **11b**, Et_3N, CH_2Cl_2.

Inhibitors **3a–e** were first evaluated in enzyme inhibitory assay utilizing the protocol described by Toth and Marshall.[20] Compounds that showed potent enzymatic K_i values were then further evaluated in antiviral assay. The inhibitor structure and potency are shown in Table 1. As shown, incorporation of a stereochemically defined 3(*S*)-tetrahydrofuran ring as the P2-ligand provided inhibitor **3a**, which displayed an enzyme inhibitory potency of 0.2 nM and antiviral IC_{50} value of 20 nM. The corresponding derivative **14a** with a hydroxyethylamine isostere exhibited over 400-fold reduction in enzyme inhibitory activity. Introduction of a stereochemically defined bis-THF as the P2-ligand, resulted in inhibitor **3b**, which displayed over 40-fold potency enhancement with respect to **3a**. Inhibitor **3b** displayed a K_i of 5.2 pM in the enzyme inhibitory assay. Furthermore, compound **3b** has shown an impressive antiviral activity with an IC_{50} value of 9 nM. Inhibitor **14b** with hydroxyethylamine isostere is significantly less potent than the corresponding norstatine-derived inhibitor **3b**. Inhibitor **3c** with a (3a*S*, 5*R*, 6a*R*)-5-hydroxy-hexahydrocyclopenta[*b*]furan as the P2-ligand has displayed excellent inhibitory activity, and particularly, antiviral activity, showing an IC_{50} value of 13 nM. Other structure-based designed ligands in inhibitors **3d** and **3e** have shown subnanomolar enzyme inhibitory activity. However, inhibitor **3b** with a bis-THF ligand has shown the most impressive activity.

To obtain molecular insight into the possible ligand-binding site interactions, we have created energy-minimized models of a number of inhibitors based upon protein-ligand X-ray structure of KNI-764 (**2**).[21] An overlayed model of **3b** with the X-ray structure of **2**-bound HIV-1 protease is shown in Figure 2. This model for inhibitor **3b** was created from the X-ray crystal structure of KNI-764 (**2**)-bound HIV-1 protease (KNI-764, pdb code 1MSM[21]) and the X-ray crystal structure of darunavir (pdb code 2IEN[22]), by combining the P2-end of the darunavir structure with the P2′-end of the KNI-764 structure, followed by 1000 cycles of energy minimization. It appears that both oxygens of the bis-THF ligand are suitably located to form hydrogen bonds with the backbone atoms of Asp-29 and Asp-30 NH's, similar to darunavir-bound HIV-1 protease.[10] Furthermore, the KNI-764-X-ray structure-derived model of **3b** suggested that the incorporation of appropriate substituents on the phenyl ring could interact with Asp-29′ and Asp-30′ in the S2′-subsite. In particular, it appears that a 4-hydroxymethyl substituent on the P2′-phenyl ring could conceivably interact with backbone Asp-30′ NH in the S2′-subsite. Other substituents such as a methoxy group or an amine functionality also appears to be within proximity to Asp-29′ and Asp-30′ backbone NHs. Based upon these speculations, we incorporated *p*-MeO, *p*-NH_2 and *p*-CH_2OH substituents on the P2′-phenyl ring of inhibitor **3b**. As shown in Table 1, neither *p*-MeO nor *p*-NH_2 groups improved enzyme inhibitory potency compared to inhibitor **3b**. Of particular note, compound **16a**, displayed a good antiviral potency, possibly suggesting a better penetration through the cell membrane. Inhibitor **16c** with a hydroxymethyl substituent showed sub-nanomolar enzyme inhibitory potency but its antiviral activity was moderate compared to unsubstituted derivative **3b**. As it turned out, inhibitor **3b** is the most potent inhibitor in the series. We subsequently examined its activity against a clinical wild-type X_4-HIV-1 isolate (HIV-$1_{ERS104pre}$) along with various multidrug-resistant clinical X_4- and R_5- HIV-1 isolates using PBMCs as target cells.[5b] As can be seen in Table 2, the potency of **3b** against HIV-$1_{ER104pre}$ (IC_{50} = 31 nM) was comparable to the FDA approved PI, amprenavir with an IC_{50} value of 45 nM. Darunavir and atazanavir on the other hand, are significantly more potent with IC_{50} values of 5 nM and 3 nM, respectively. Inhibitor **3b**, while less potent than darunavir, maintained 5-fold or better potency over amprenavir against HIV-$1_{MDR/C}$, HIV-$1_{MDR/G}$, HIV-$1_{MDR/TM}$ and HIV-$1_{MDR/MM}$. It maintained over a 2-fold potency against HIV-$1_{MDR/JSL}$. In fact, inhibitor **3b** maintained comparable potency to atazanavir against all

Table 1
Enzymatic inhibitory and antiviral activity of allophenylnorstatine-derived inhibitors

Entry	Inhibitor	K_i (nM)	$IC_{50}^{a,b}$ (μM)
1	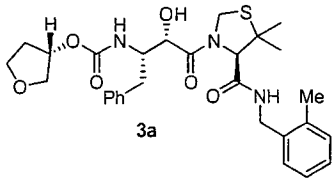 3a	0.21	0.02
2	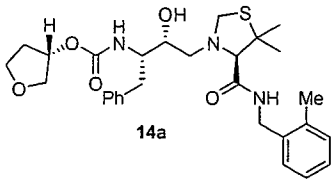 14a	86.2	nt
3	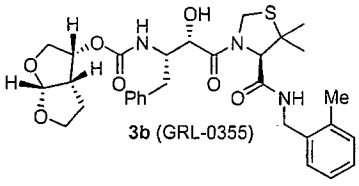 3b (GRL-0355)	0.0052	0.009
4	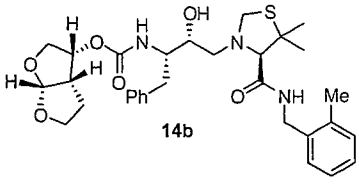 14b	2.6	nt
5	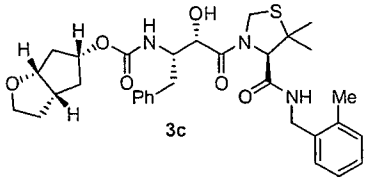 3c	0.29	0.013
6	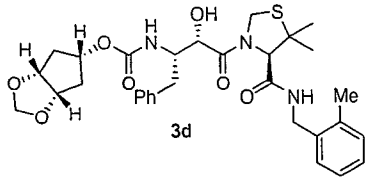 3d	0.65	nt
7	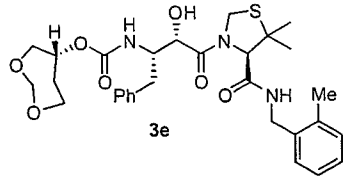 3e	0.78	nt
8	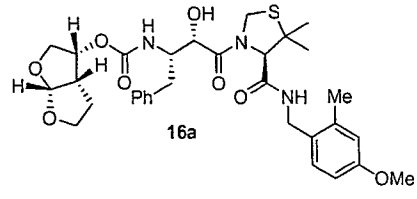 16a	2.03	0.051

Table 1 (*continued*)

Entry	Inhibitor	K_i (nM)	IC_{50}[a,b] (μM)
9	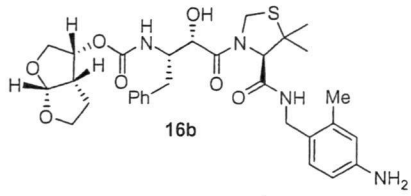 16b	1.01	0.53
10	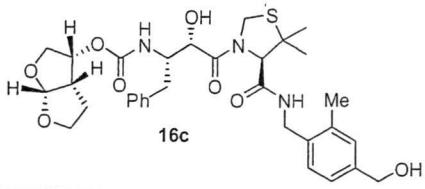 16c	0.31	0.23

[a] Values are means of at least three experiments.
[b] Human lymphoid (MT-2) cells were exposed to 100 $TCID_{50}$ values of HIV-1_{LAI} and cultured in the presence of each PI, and IC_{50} values were determined using MTT assay. Darunavir exhibited K_i = 16 pM, IC_{50} = 1.6 nM.

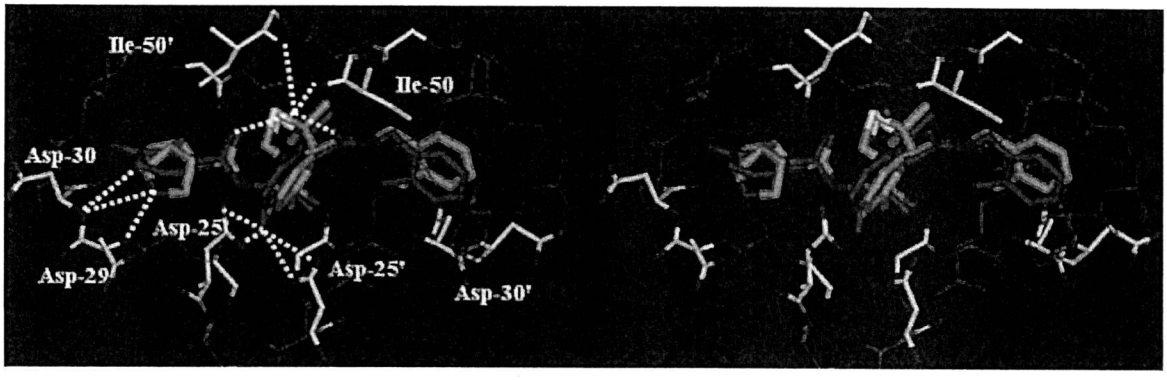

Figure 2. Structure of inhibitor **3b**, modeled into the active site of HIV-1 protease, superimposed on the X-ray crystal structure of KNI-764. Inhibitor **3b** carbons are shown in green and KNI-764 carbons are shown in magenta.

Table 2
Antiviral activity of **3b** (GRL-0355) against multidrug-resistant clinical isolates in PHA-PBMs.

Virus	IC_{50} (μM)			
	3b (GRL-0355)	APV	ATV	DRV
HIV-$1_{ERS104pre}$ (wild-type: X4)	0.031 ± 0.002	0.045 ± 0.014	0.003 ± 0.003	0.005 ± 0.001
HIV-$1_{MDR/C}$ (X4)	0.061 ± 0.005 (2)	0.346 ± 0.071 (8)	0.045 ± 0.026 (15)	0.010 ± 0.006 (2)
HIV-$1_{MDR/G}$ (X4)	0.029 ± 0.002 (1)	0.392 ± 0.037 (9)	0.029 ± 0.020 (10)	0.019 ± 0.005 (4)
HIV-$1_{MDR/TM}$ (X4)	0.064 ± 0.032 (2)	0.406 ± 0.082 (9)	0.047 ± 0.009 (16)	0.007 ± 0.003 (1)
HIV-$1_{MDR/MM}$ (R5)	0.042 ± 0.001 (1)	0.313 ± 0.022 (7)	0.040 ± 0.002 (13)	0.027 ± 0.008 (5)
HIV-$1_{MDR/JSL}$ (R5)	0.235 ± 0.032 (8)	0.531 ± 0.069 (12)	0.635 ± 0.065 (212)	0.028 ± 0.008 (6)

The amino acid substitutions identified in the protease-encoding region of HIV-$1_{ERS104pre}$, HIV-1_C, HIV-1_G, HIV-1_{MM}, HIV-1_{JSL} compared to the consensus type B sequence cited from the Los Alamos database include L63P; L10I, I15V, K20R, L24I, M36I, M46L, I54V, I62V, L63P, K70Q,V82A, L89M; L10I, V11I, T12E, I15V, L19I, R41K, M46L, L63P, A71T, V82A, L90M; L10I, K14R, R41K, M46L, I54V, L63P, A71V, V82A, L90M; L10I, K43T, M46L, I54V, L63P, A71V, V82A, L90M, Q92K; and L10I, L24I, I33F, E35D, M36I, N37S, M46L, I54V, R57K, I62V, L63P, A71V, G73S, V82A, respectively. HIV-$1_{ERS104pre}$ served as a source of wild-type HIV-1. The IC_{50} values were determined by using PHA-PBMs as target cells and the inhibition of p24 Gag protein production by each drug was used as an endpoint. The numbers in parentheses represent the fold changes of IC_{50} values for each isolate compared to the IC_{50} values for wild-type HIV-$1_{ERS104pre}$. All assays were conducted in duplicate, and the data shown represent mean values (±1 standard deviations) derived from the results of two or three independent experiments. Amprenavir = APV; Atazanavir = ATV; Darunavir = DRV.

multidrug-resistant clinical isolates tested. The reason for its impressive potency against multidrug-resistant clinical isolates is possibly due to its ability to make extensive hydrogen-bonds with the protease backbone in the S2 subsite and its ability to fill in the hydrophobic pockets in the S1′–S2′ subsites effectively.

In conclusion, incorporation of stereochemically defined and conformationally constrained cyclic ethers into the allophenylnorstatine resulted in a series of potent protease inhibitors. The promising inhibitors **3b** and **3c** are currently being subjected to further in-depth biological studies. Design and synthesis of new

classes of inhibitors based upon above molecular insight are currently ongoing in our laboratories.

Acknowledgement

The financial support of this work is provided by the National Institute of Health (GM 83356).

References and notes

1. Sepkowitz, K. A. *N. Eng. J. Med.* **2001**, *344*, 1764–1772.
2. Kohl, N. E.; Emini, E. A.; Schleif, W. A.; Davis, L. J.; Heimbach, J. C.; Dixon, R. A. F.; Scolnick, E. M.; Sigal, I. S. *Proc. Natl. Acad. Sci. U.S.A.* **1988**, *85*, 4686–4690.
3. (a) Pillay, D.; Bhaskaran, K.; Jurriaans, S.; Prins, M.; Masquelier, B.; Dabis, F.; Gifford, R.; Nielsen, C.; Pedersen, C.; Balotta, C.; Rezza, G.; Ortiz, M.; de Mendoza, C.; Kücherer, C.; Poggensee, G.; Gill, J.; Porter, K. *AIDS* **2006**, *20*, 21–28; (b) Grabar, S.; Pradier, C.; Le Corfec, E.; Lancar, R.; Allavena, C.; Bentata, M.; Berlureau, P.; Dupont, C.; Fabbro-Peray, P.; Poizot-Martin, I.; Costagliola, D. *AIDS* **2000**, *14*, 141–149.
4. Wainberg, M. A.; Friedland, G. *JAMA* **1998**, *279*, 1977–1983.
5. (a) Ghosh, A. K.; Kincaid, J. F.; Cho, W.; Walters, D. E.; Krishnan, K.; Hussain, K. A.; Koo, Y.; Cho, H.; Rudall, C.; Holland, L.; Buthod, J. *Bioorg. Med. Chem. Lett.* **1998**, *8*, 687–690; (b) Koh, Y.; Maeda, K.; Ogata, H.; Bilcer, G.; Devasamudram, T.; Kincaid, J. F.; Boross, P.; Wang, Y.-F.; Tie, Y.; Volarath, P.; Gaddis, L.; Louis, J. M.; Harrison, R. W.; Weber, I. T.; Ghosh, A. K.; Mitsuya, H. *Antimicrob. Agents Chemother.* **2003**, *47*, 3123–3129; (c) Ghosh, A. K.; Pretzer, E.; Cho, H.; Hussain, K. A.; Duzgunes, N. *Antiviral Res.* **2002**, *54*, 29–36.
6. Yoshimura, K.; Kato, R.; Kavlick, M. F.; Nguyen, A.; Maroun, V.; Maeda, K.; Hussain, K. A.; Ghosh, A. K.; Gulnik, S. V.; Erickson, J. W.; Mitsuya, H. *J. Virol.* **2002**, *76*, 1349–1358.
7. Ghosh, A. K.; Sridhar, P. R.; Leshchenko, S.; Hussain, A. K.; Li, J.; Kovalevsky, A. Y.; Walters, D. E.; Wedekind, J. K.; Grum-Tokars, V.; Das, D.; Koh, Y.; Maeda, K.; Gatanaga, H.; Weber, I. T.; Mitsuya, H. *J. Med. Chem.* **2006**, *49*, 5252.
8. Koh, Y.; Das, D.; Leshchenko, S.; Nakata, H.; Ogata-Aoki, H.; Amano, M.; Nakayama, M.; Ghosh, A. K.; Mitsuya, H. *Antimicrob. Agents Chemother.* **2009**, *53*, 997–1006.
9. (a) FDA approved Darunavir on June 23, 2006: FDA approved new HIV treatment for patients who do not respond to existing drugs. Please see: http://www.fda.gov/NewsEvents/Newsroom/PressAnnouncements/2006/ucm108676.htm (b) On October 21, 2008, FDA granted traditional approval to Prezista (darunavir), co-administered with ritonavir and with other antiretroviral agents, for the treatment of HIV-1 infection in treatment-experienced adult patients. In addition to the traditional approval, a new dosing regimen for treatment-naïve patients was approved.
10. Ghosh, A. K.; Chapsal, B. D.; Weber, I. T.; Mitsuya, H. *Acc. Chem. Res.* **2008**, *41*, 78–86.
11. Ghosh, A. K.; Ramu Sridhar, P.; Kumaragurubaran, N.; Koh, Y.; Weber, I. T.; Mitsuya, H. *ChemMedChem* **2006**, *1*, 939–950.
12. Mimoto, T.; Terashima, K.; Nojima, S.; Takaku, H.; Nakayama, M.; Shintani, M.; Yamaoka, T.; Hayashi, H. *Bioorg. Med. Chem.* **2004**, *12*, 281–293.
13. Yoshimura, K.; Kato, R.; Yusa, K.; Kavlick, M. F.; Maroun, V.; Nguyen, A.; Mimoto, T.; Ueno, T.; Shintani, M.; Falloon, J.; Masur, H.; Hayashi, H.; Erickson, J.; Mitsuya, H. *Proc. Natl. Acad. Sci. U.S.A.* **1999**, *96*, 8675–8680.
14. Ghosh, A. K.; Thompson, W. J.; Holloway, M. K.; McKee, S. P.; Duong, T. T.; Lee, H. Y.; Munson, P. M.; Smith, A. M.; Wai, J. M.; Darke, P. L.; Zugay, J.; Emini, E. A.; Schleif, W. A.; Huff, J. R.; Anderson, P. S. *J. Med. Chem.* **1993**, *36*, 2300–2310.
15. Ohmoto, K.; Okuma, M.; Yamamoto, T.; Kijima, H.; Sekioka, T.; Kitagawa, K.; Yamamoto, S.; Tanaka, K.; Kawabata, K.; Sakata, A., et al *Bioorg. Med. Chem. Lett.* **2001**, *9*, 1307–1323.
16. Ikunaka, M.; Matsumoto, J.; Nishimoto, Y. *Tetrahedron: Asymmetry* **2002**, *13*, 1201–1208.
17. Iwona Kudyba, I.; Raczko, J.; Jurczak, J. *J. Org. Chem.* **2004**, *69*, 2844–2850.
18. Ghosh, A. K.; Duong, T. T.; McKee, S. P. *Tetrahedron Lett.* **1992**, *33*, 2781–2784.
19. (a) Ghosh, A. K.; Leshchenko, S.; Noetzel, M. *J. Org. Chem.* **2004**, *69*, 7822–7829; (b) Ghosh, A. K.; Gemma, S.; Takayama, J.; Baldridge, A.; Leshchenko-Yashchuk, S.; Miller, H. B.; Wang, Y.-F.; Kovalevsky, A. Y.; Koh, Y.; Weber, I. T.; Mitsuya, H. *Org. Biomol. Chem.* **2008**, *6*, 3703–3713; (c) Ghosh, A. K.; Gemma, S.; Baldridge, A.; Wang, Y.-F.; Kovalevsky, A. Y.; Koh, Y.; Weber, I. T.; Mitsuya, H. *J. Med. Chem.* **2008**, *51*, 6021–6033.
20. Toth, M. V.; Marshall, G. R. A. *Int. J. Pep. Protein Res.* **1990**, *36*, 544–550.
21. Vega, S.; Kang, L.-W.; Velazquez-Campoy, A.; Kiso, Y.; Amzel, L. M.; Freire, E. *Proteins* **2004**, *55*, 594–602.
22. Kovalevski, A. Y.; Louis, J. M.; Aniana, A.; Ghosh, A. K.; Weber, I. T. *J. Mol. Biol.* **2008**, *384*, 178–192.

Design of HIV-1 Protease Inhibitors with Pyrrolidinones and Oxazolidinones as Novel P1′-Ligands To Enhance Backbone-Binding Interactions with Protease: Synthesis, Biological Evaluation, and Protein–Ligand X-ray Studies[∞]

Arun K. Ghosh,*,† Sofiya Leshchenko-Yashchuk,† David D. Anderson,† Abigail Baldridge,† Marcus Noetzel,† Heather B. Miller,† Yunfeng Tie,‡ Yuan-Fang Wang,‡ Yasuhiro Koh,⊥ Irene T. Weber,‡ and Hiroaki Mitsuya[||,⊥]

Departments of Chemistry and Medicinal Chemistry, Purdue University, West Lafayette, Indiana 47907, Department of Biology, Molecular Basis of Disease, Georgia State University, Atlanta, Georgia 30303, Departments of Hematology and Infectious Diseases, Kumamoto University School of Medicine, Kumamoto 860-8556, Japan, and Experimental Retrovirology Section, HIV and AIDS Malignancy Branch, National Cancer Institute, Bethesda, Maryland 20892

Received March 10, 2009

Structure-based design, synthesis, and biological evaluation of a series of novel HIV-1 protease inhibitors are described. In an effort to enhance interactions with protease backbone atoms, we have incorporated stereochemically defined methyl-2-pyrrolidinone and methyl oxazolidinone as the P1′-ligands. These ligands are designed to interact with Gly-27′ carbonyl and Arg-8 side chain in the S1′-subsite of the HIV protease. We have investigated the potential of these ligands in combination with our previously developed bis-tetrahydrofuran (bis-THF) and cyclopentanyltetrahydrofuran (Cp-THF) as the P2-ligands. Inhibitor **19b** with a (*R*)-aminomethyl-2-pyrrolidinone and a Cp-THF was shown to be the most potent compound. This inhibitor maintained near full potency against multi-PI-resistant clinical HIV-1 variants. A high resolution protein–ligand X-ray crystal structure of **19b**-bound HIV-1 protease revealed that the P1′-pyrrolidinone heterocycle and the P2-Cp-ligand are involved in several critical interactions with the backbone atoms in the S1′ and S2 subsites of HIV-1 protease.

Introduction

Advances in the treatment of HIV[a]/AIDS with HIV-1 protease inhibitors in combination with reverse transcriptase inhibitors have been widely documented.[1] The combination therapy, also known as highly active antiretroviral therapy (HAART), blocks critical viral replication at two different stages of the replication cycle.[2] The HAART regimens have resulted in dramatic reduction of blood plasma viral load levels, increased CD_4^+ lymphocyte counts, and improved life expectancy and significantly reduced HIV/AIDS-related mortality in the developed world.[3] Despite these important advances, effective long-term suppression of HIV infection with HAART regimens is a complex issue in medicine for a number of reasons. These include drug side effects, poor penetration into protected HIV reservoir sites, poor oral bioavailability, and interactions between drugs.[4] Perhaps one of the most daunting problems in future management of HIV is the emergence of drug-resistant HIV-1 variants and the transmission of these viral strains.[5,6] Thus, development of antiretroviral therapy with broad-spectrum activity and minimal drug side effects is critical for an effective management of current and future HIV/AIDS treatment. We recently reported the design and development of a number of exceedingly potent nonpeptidic HIV-1 protease inhibitors (PIs) **1**–**3** (Figure 1).[7–9] One of those PIs is darunavir (**1**, TMC-114), which was approved by the FDA in 2006 for the treatment of HIV/AIDS patients who are harboring drug-resistant HIV and do not respond to other therapies.[10] More recently, darunavir has received full approval for all HIV/AIDS patients.[11]

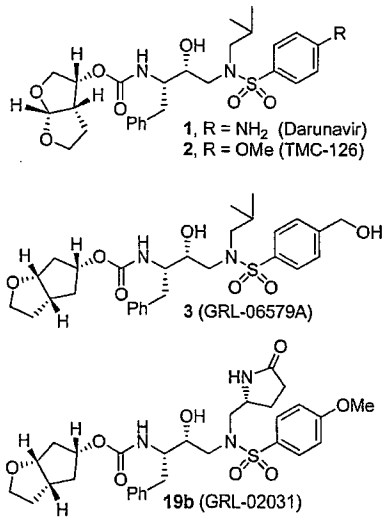

Figure 1. Structures of inhibitors **1**–**3** and **19b**.

To combat drug resistance, our structure-based design strategies are to maximize the protease active-site interactions with the inhibitor and particularly to promote extensive hydrogen bonding with the protein backbone atoms.[12] It is evident that active site backbone conformation of mutant proteases is only minimally distorted compared to that of the wild-type HIV-1 protease.[13,14] Therefore, the "backbone binding" strategy may be important to combat drug resistance.[12] Using high resolution protein–ligand X-ray structures of **1**- and **3**-bound HIV-1

[∞] The PDB accession code for **19b**-bound HIV-1 protease X-ray structure is 3H5B.

* To whom correspondence should be addressed. Phone: (765) 494-5323. Fax: (765) 496-1612. E-mail: akghosh@purdue.edu.
† Purdue University.
‡ Georgia State University.
⊥ Kumamoto University School of Medicine.
|| National Cancer Institute.

[a] Abbreviations: HIV, human immunodeficiency virus; bis-THF, bis-tetrahydrofuran; Cp-THF, cyclopentanyltetrahydrofuran; PI, protease inhibitor; HAART, highly active antiretroviral therapy; APV, amprenavir; DRV, darunavir; SQV, saquinavir; IDV, indinavir; LPV, lopinavir; RTV, ritonavir.

10.1021/jm900303m CCC: $40.75
Published on Web 05/27/2009

Scheme 1. Synthesis of Lactam Containing Sulfonamide Isosteres

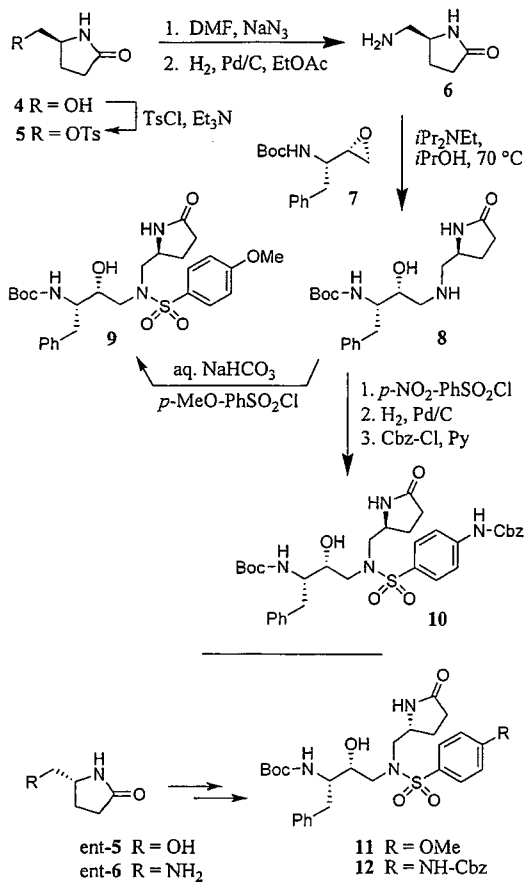

Scheme 2. Synthesis of Lactam Containing PIs

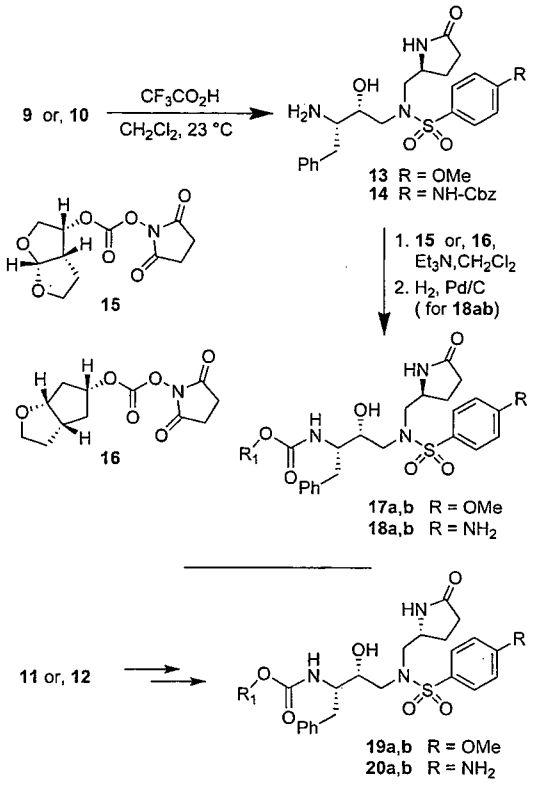

protease, we have shown that these PIs were engaged in extensive hydrogen bonding interactions with the backbone atoms throughout the active site cavity from the S2 to S2′ regions.[9,15] To further enhance "backbone binding" interactions, we became interested in designing an appropriately functionalized P1′-ligand that could interact with the backbone atoms, particularly with the Gly-27′ and Arg-8 in the S1′-subsite. This enhancement of "backbone binding" interaction may lead to inhibitors with improved drug-resistance profiles. Herein, we report the design, synthesis, and biological evaluation of a series of potent HIV-1 protease inhibitors that incorporated structure-based designed stereochemically defined lactam and oxazolidinone derivatives as the P1′-ligands in combination with the bis-THF or Cp-THF as the P2-ligands. Inhibitor **19b** incorporating a (*R*)-5-aminomethyl-2-pyrrolidinone as the P1′-ligand and Cp-THF as the P2-ligand is the most potent PI in the series. Interestingly, this PI has retained full potency against a range of multidrug-resistant HIV-1 variants. The protein−ligand X-ray structure of **19b**-bound HIV-1 protease revealed important molecular insight into the ligand-binding site interactions.

Chemistry

The optically active synthesis of the requisite 5-aminomethyl-2-pyrrolidinone for P1-ligands and their conversion to respective sulfonamide isostere are shown in Scheme 1. Commercially available 5-(*S*)-hydroxymethyl-2-pyrrolidinone **4** was reacted with tosyl chloride and triethylamine to provide tosylate **5**. Displacement of the tosylate with sodium azide in DMF at 55 °C for 9 h provided the azide derivative in 92% yield over two steps. Catalytic hydrogenation of the azide over 10% Pd−C in ethyl acetate afforded optically active amine **6** in quantitative yield. 5-(*R*)-Hydroxymethyl-2-pyrrolidinone (*ent*-**5**) was similarly converted to optically active amine *ent*-**6** in comparable yield. Amine **6** was reacted with commercially available epoxide **7** in the presence of *i*-Pr_2NEt (DIPEA) in 2-propanol at 70 °C for 36 h to provide epoxide-opened product **8** in 85% yield.[16] Amine **8** was converted to *p*-methoxybenezenesulfonamide derivative **9** by reaction with *p*-methoxybenzenesulfonyl chloride in the presence of aqueous $NaHCO_3$ in quantitative yield. Treatment of amine **8** with *p*-nitrobenzenesulfonyl chloride afforded the corresponding nitrosulfonamide. Catalytic hydrogenation over 10% Pd−C gave the corresponding aniline derivative, which was reacted with benzyl chloroformate in the presence of pyridine to furnish Cbz-derivative **10** in 63% yield for three steps. Enantiomeric amine (*ent*-**6**) was converted to the respective methoxy and Cbz-derived **11** and **12** by analogous procedures.

The synthesis of various PIs incorporating methylpyrrolidinones as the P1′-ligand is shown in Scheme 2. Exposure of Boc-derivatives **9** and **10** to 30% CF_3CO_2H in CH_2Cl_2 at 23 °C for 40 min resulted in the respective amines **13** and **14**. Alkoxycarbonylation of amine **13** with activated mixed carbonates **15**[16] and **16**[9] in the presence of Et_3N in CH_2Cl_2 furnished inhibitors **17a** and **17b** in 98% and 87% yields, respectively.[17] Alkoxycarbonylation of amine **14** with activated carbonates **15** and **16** afforded the corresponding Cbz-protected urethanes. Removal of the Cbz-group by catalytic hydrogenation over 10% Pd−C in ethyl acetate provided inhibitor **18a** and **18b** in 58% and 62% yields, respectively. Sulfonamide derivatives **11** and **12** containing enantiomeric P1′-ligands were converted to inhibitors **19a,b** and **20a,b** by following analogous procedures.

The synthesis of sulfonamide isosteres incorporating methyloxazolidinone as the P1′-ligand is shown in Scheme 3. Optically

Scheme 3. Synthesis of Sulfonamide Isosteres with P_1'-Oxazolidinone

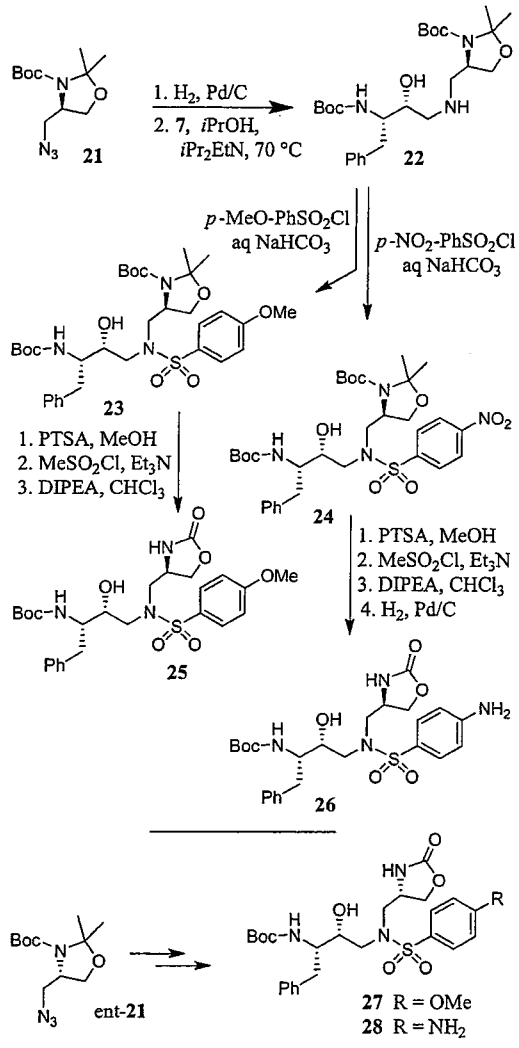

active dimethyloxazolidines **21** and *ent*-**21** were prepared by following the procedure described by Dondini and co-workers.[18] Reduction of these azides by catalytic hydrogenation in methanol afforded the respective amine. Reaction of **21**-derived amine with epoxide **7** in the presence of *i*-Pr_2NEt in 2-propanol afforded amine **22** in 41% yield. Reaction of amine **22** with *p*-methoxybenzenesulfonyl chloride or *p*-nitrobenzenesulfonyl chloride as described previously afforded sulfonamide derivatives **23** and **24** in 80% and 92% yields, respectively. The isopropylidene functionality in **23** and **24** was converted to the corresponding oxazolidinone derivative in a three-step sequence involving (1) treatment of **23** by a catalytic amount of *p*-toluenesulfonic acid (PTSA) in methanol, resulting in the removal of the isopropylidene group, (2) reaction of the resulting Boc-amino alcohol with mesyl chloride in the presence of triethylamine to provide the corresponding mesylate, and (3) treatment of the resulting mesylate with *i*-Pr_2NEt in chloroform at reflux. This has provided oxazolidinone **25** in 45% yield over three steps. The nitrosulfonamide derivative **24** was similarly converted to the corresponding oxazolidinone. Catalytic hydrogenation of the resulting nitro derivative with 10% Pd−C in methanol provided aniline derivative **26** in 37% overall yield

Scheme 4. Synthesis of Oxazolidinone-Derived PIs

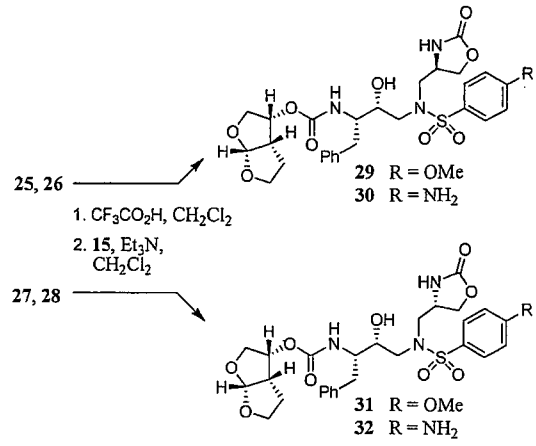

over four steps. Enantiomeric azide *ent*-**21** was converted to oxazolidinone derivatives **27** and **28** by following analogous procedures.

The synthesis of inhibitors containing oxazolidinone as P1′-ligand and bis-THF as the P2-ligand is shown in Scheme 4. Treatment of oxazolidinones **25**−**28** with 30% CF_3CO_2H in CH_2Cl_2 at 23 °C afforded the corresponding amines. Reaction of the resulting amines with activated mixed carbonate **15** in the presence of Et_3N in CH_2Cl_2 afforded the target inhibitors **29**−**32** in excellent yields (80−90%). The structures of these inhibitors are shown in Table 1.

Results and Discussion

Our examination of the X-ray structure of **1**-bound HIV-1 protease and its respective modeling initially suggested that a methyl-2-pyrrolidinone may interact well with residues in the S1′-site.[15] As shown in Table 1, our first set of inhibitors contain a (*R*)-hydroxyethylamine sulfonamide isostere with either the bis-THF or Cp-THF as the P2-ligand and *p*-methoxysulfonamide or *p*-aminosulfonamide as the P2′-ligand. The enzyme inhibitory potency of these PIs was evaluated according to the procedure reported by Toth and Marshall.[19] Inhibitor **17a** with (*S*)-methyl-2-pyrrolidinone displayed an enzyme K_i of 1 nM. Inhibitor **17b** with a Cp-THF showed a 3-fold improvement of potency. Antiviral activity of these inhibitors was determined in MT-2 human T-lymphoid cells exposed to HIV-1_{LAI}. Interestingly, both inhibitors have shown dramatic reduction in antiviral activity. Inhibitors **17a** and **17b** have shown IC_{50} values of 0.48 and 0.23 μM, respectively. However, these inhibitors are significantly less potent compared to inhibitors with an isobutyl group as the P1′-ligand.[7c,9] Incorporation of *p*-aminosulfonamide (PIs **18a** and **18b**) as the P2′-ligand led to a drop in enzyme inhibitory as well as antiviral potency. Inhibitor **19a** containing (*R*)-methyl-2-pyrrolidinone as the P1′-ligand has shown 10-fold enhancement of enzyme K_i over the (*S*)-isomer **17a**. It showed a slight improvement in antiviral activity compared to inhibitor **17a**. Inhibitor **19b** with (*R*)-methyl-2-pyrrolidinone as the P1′-ligand and Cp-THF as the P2-ligand resulted in the most potent inhibitor in the series. It has shown an enzymatic K_i of 99 pM and a 10-fold improvement (IC_{50} = 0.026 μM) in antiviral activity relative to epimeric (*S*)-pyrrolidinone derivative **17b**, suggesting an important role for the P1′-ring stereochemistry. Indeed, an X-ray structure of **19b**-bound HIV-1 protease revealed that the pyrrolidinone carbonyl and the NH functionalities were positioned to hydrogen-bond with residues in the S1′-site. Interestingly, the combination of P1′-methylpyrrolidi-

Table 1. Enzymatic Inhibitory Activity of Lactam and Oxazolidinone Containing Inhibitors[b]

Entry	Inhibitor	K_i(nM)	IC_{50}(nM)[a]
1.	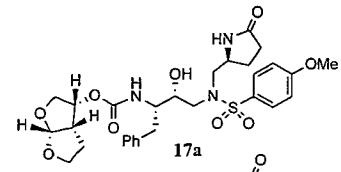 **17a**	0.85±0.02	0.48±0.05
2.	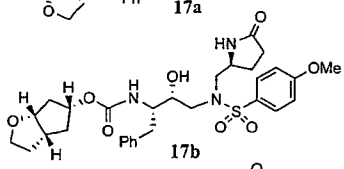 **17b**	0.31±0.03	0.23±0.08
3.	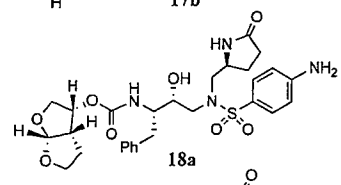 **18a**	0.28±0.03	>1
4.	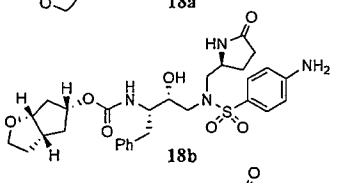 **18b**	1.27±0.15	>1
5.	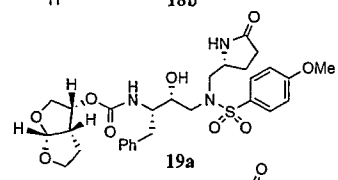 **19a**	0.12±0.003	0.25±0.11
6.	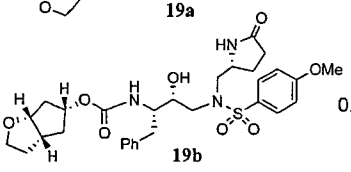 **19b**	0.099±0.003	0.026±0.002
7.	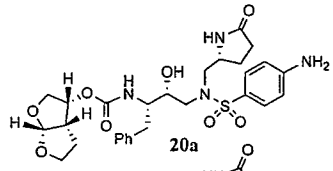 **20a**	0.85±0.2	>1
8.	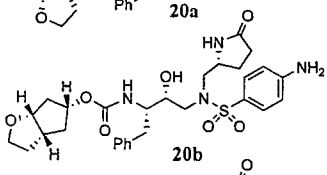 **20b**	0.31±0.03	0.60±0.24
9.	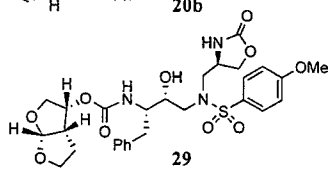 **29**	0.28±0.03	0.48±0.17
10.	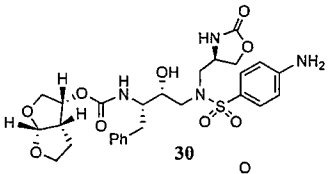 **30**	0.31±0.03	>1
11.	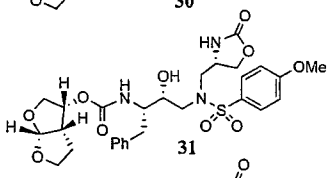 **31**	0.035±0.01	0.31±0.21
12.	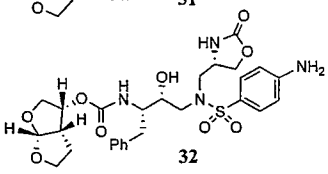 **32**	0.24±0.03	>1

[a] Values are the mean of at least two experiments. [b] Human T-lymphoid (MT-2) cells (2×10^3) were exposed to 100 $TCID_{50}$ values of HIV-1_{LAI} and cultured in the presence of each PI, and IC_{50} values were determined using the MTT assay. The IC_{50} values of amprenavir (APV), saquinavir (SQV), and indinavir (IDV) were 0.03, 0.015, and 0.03 μM, respectively.

none and polar P2′-*p*-aminosulfonamide led to PIs with subnanomolar enzyme activity. However, antiviral activity was reduced drastically. In PIs **29**−**32**, we have incorporated both (*S*)- and (*R*)-oxazolidinone derivatives as substitutes for the respective pyrrolidinone isomers. As can be seen, oxazolidinone derivatives **29**−**32** have shown subnanomolar enzyme inhibitory potency. Inhibitors with *p*-methoxysulfonamide as the P2′-ligand displayed comparable antiviral activity relative to pyrrolidinone derivatives. Consistent with stereochemical preference, the (*R*)-oxazolidinone with *p*-methoxysulfonamide has shown better enzyme K_i values. However, the antiviral activity of these compounds is very similar. In general, both pyrrolidinone and oxazolidinone functionalities appear to be nicely accommodated in the S1′-site.

While inhibitor **31** is very potent in enzyme inhibitory assay, the significant reduction of antiviral potency is possibly due to poor cellular permeability of this polar functionality. Inhibitor **19b** appeared to be most potent among the series of inhibitors examined. It exhibited comparable antiviral activity with the FDA approved PIs amprenavir, saquinavir, and indinavir in the same assay.

Inhibitor **19b** was subsequently examined for its activity against a clinical wild-type X_4-HIV-1 isolate (HIV-$1_{ERS104pre}$) along with various multidrug-resistant clinical X_4- and R_5-HIV-1 isolates using PBMCs as target cells.[8b] As can be seen in Table 2, the potency of **19b** against HIV-$1_{ER104pre}$ (IC_{50} = 28 nM) was comparable to FDA approved PIs indinavir, amprenavir, and lopinavir with IC_{50} values of 28, 25, and 30 nM, respectively. Darunavir, on the other hand, is nearly 10-fold more potent (IC_{50} = 3.6 nM) than **19b** and the above-mentioned PIs. Interestingly, of all the PIs tested, indinavir was least able to suppress the replication of the multidrug-resistant clinical isolate examined (HIV-$1_{MDR/MM}$, HIV-$1_{MDR/TM}$, HIV-$1_{MDR/C}$, and HIV-$1_{MDR/G}$) with IC_{50} values greater than 1 μM. Both amprenavir and lopinavir displayed 10-fold or greater reduction in potency except against HIV-1MDR/G, where lopinavir showed a 5-fold reduction in potency. A more detailed virologic study using inhibitor **19b** will be published elsewhere.[20] Darunavir has maintained impressive activity against all the multidrug-resistant variants. Inhibitor **19b**, while less potent than darunavir, maintained near full potency against multidrug-resistant clinical isolates examined. This impressive drug-resistance property of **19b** is possibly due to its extensive interactions, particularly its ability to make extensive hydrogen bonding throughout the active site of the protease's backbone. Furthermore, inhibitor **19b** blocked the infection and replication

Table 2. Anti-HIV Activity of **19b** against Selected Clinical Isolates Highly Resistant to Multiple Protease Inhibitors[a]

virus	phenotype	EC_{50} (μM)				
		IDV	APV	LPV	DRV	**19b**
HIV-$1_{ERS104pre}$ (wild-type)	X4	0.028 ± 0.005	0.025 ± 0.006	0.03 ± 0.001	0.0036 ± 0.0002	0.028 ± 0.004
HIV-1_{TM} (MDR)	X4	>1 (>36)	0.25 ± 0.02 (10)	0.73 ± 0.53 (24)	0.0036 ± 0.0002 (1)	0.029 ± 0.004 (1)
HIV-1_{MM} (MDR)	R5	>1 (>36)	0.32 ± 0.03 (13)	0.72 ± 0.31 (24)	0.019 ± 0.009 (5)	0.042 ± 0.002 (2)
HIV-1_C (MDR)	X4	>1 (>36)	0.35 ± 0.03 (14)	0.32 ± 0.01 (11)	0.015 ± 0.001 (4)	0.023 ± 0.007 (1)
HIV-1_G (MDR)	X4	0.29 ± 0.07 (10)	0.33 ± 0.16 (13)	0.14 ± 0.01 (5)	0.014 ± 0.006 (4)	0.027 ± 0.001 (1)

[a] Amino acid substitutions identified in the protease-encoding regions of HIV-$1_{ERS104pre}$, HIV-1_{TM}, HIV-1_{MM}, HIV-1_C, and HIV-1_G compared to the consensus B sequence cited from the Los Alamos data base include L63P, L10I/K14R/R41K/M46L/I54V/L63P/A71V/V82A/L90M/I93L, L10I/K43T/M46L/I54V/L63P/A71V/V82A/L90M/Q92K, L10I/I15V/K20R/L24I/M36I/M46L/I54V/I62V/L63P/K70Q/V82A/L89M, and L10I/V11I/T12E/I15V/L19I/R41K/M46L/L63P/A71T/V82A/L90M, respectively. The EC_{50} values were determined by employing PHA-PBM as target cells and the inhibition of p24 *Gag* protein production as an end point. All values were determined in duplicate or triplicate, and those shown are derived from the results of three independent experiments. Numbers in parentheses represent fold changes of EC_{50} values against each isolate compared to EC_{50} values against HIV-$1_{ERS104pre}$. MDR: multidrug-resistant.

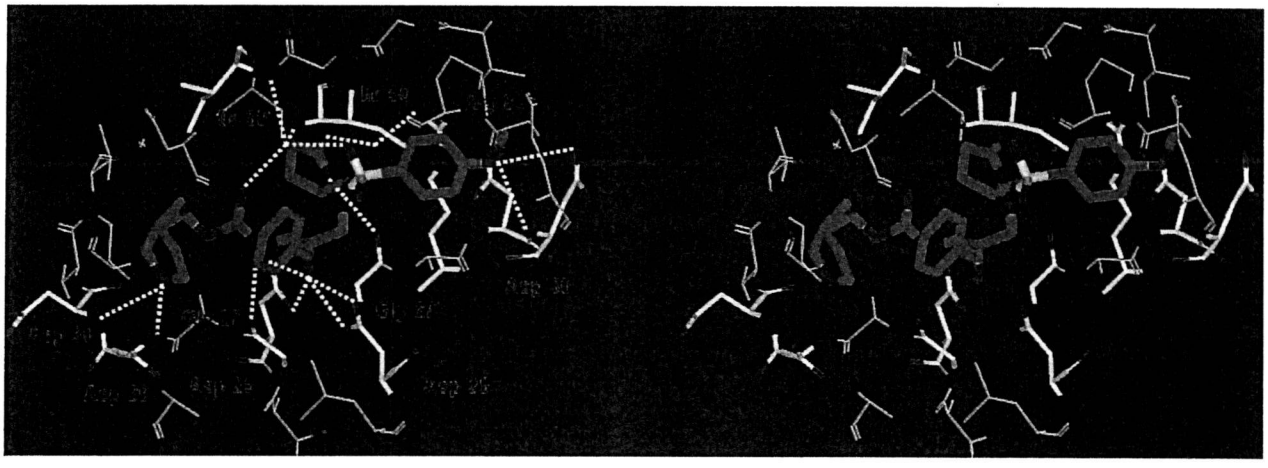

Figure 2. Stereoview of the major conformation of the X-ray structure of inhibitor **19b**-bound HIV-1 protease.

of each of the HIV-1_{NL4-3} variants exposed to and selected by up to 5 μM saquinavir, amprenavir, indinavir, nelfinavir, or ritonavir and a 1 μM lopinavir or atazanavir with EC_{50} values ranging from 0.036 to 0.14 μM.[20]

X-ray Crystallography. The binding mode of inhibitor **19b** was determined from the X-ray crystal structure of its complex with wild-type HIV-1 protease. The crystal structure was solved and refined at 1.29 Å resolution with an *R* factor of 14.1%. In this high resolution structure, the inhibitor was bound to the HIV-1 protease active site in two orientations with the relative occupancy of 0.8/0.2. The protease dimer comprises residues 1−99 and 1′−99′ of the two subunits, and the inhibitor binding site is formed by both subunits. The P1′-pyrrolidine ring also showed two alternative conformations with equal occupancy and related by about 18° rotation around the C12−C13 bond. A stereoview of the major conformation is shown in Figure 2 (only one conformation is shown for P1′). As shown, extensive interactions from P2 to P2′ were observed between the inhibitor and the protease active site, most notably favorable polar interactions including hydrogen bonds, weaker C−H···O and C−H···π interactions. The isostere hydroxyl group forms asymmetric hydrogen bonds to the carboxylate oxygen atoms of the catalytic Asp25 and Asp25′ with distances of 2.4−3.3 Å. Also, four direct hydrogen bonds are formed between the oxygens or nitrogens of the inhibitor atoms and the protease backbone atoms. These include cyclic ether oxygen of the P2-Cp-THF and the Asp-29 NH, the urethane NH with the carbonyl oxygen of Gly-27, P2′-methoxy oxygen and Asp-30′ NH. One conformation of the P1′-pyrrolidinone formed a hydrogen bond between the NH and the carbonyl oxygen of Gly-27′ and a water-mediated hydrogen bond between the P1′-pyrrolidinone carbonyl and the side chain of Arg-8. The other conformation of the P1′ group formed hydrophobic and C−H···O interactions with Pro-81′ and Val-82′, as shown in Figure 3. Also, there exists a tetracoordinated water-mediated interaction where the amides of Ile50 and Ile50′ donate hydrogen bonds, and the inhibitor's urethane carbonyl and one of the sulfonamide oxygen

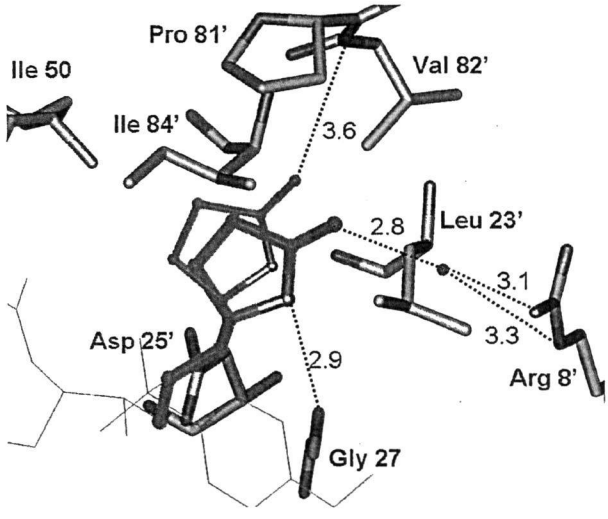

Figure 3. Protease interactions with the two alternate conformations of the inhibitor's pyrrolidine ring. The inhibitor is in green with thick bonds for the major and thin bonds for the minor conformations of the pyrrolidine ring. Hydrogen bonds are shown as dotted lines. Distances between donor and acceptor atoms are shown in Å.

accept hydrogen bonds from the water molecule. These interactions are conserved in a majority of other HIV-1 protease complexes with inhibitors[21] or substrate analogues.[22]

The weaker polar interactions such as C−H···O and water−π interactions can be analyzed accurately in this high resolution structure.[23,24] These interactions are important for inhibitor-protease binding and must be considered in the design of inhibitors. The C−H···O interactions of the inhibitor with the carbonyl oxygens of Gly-48, Gly-48′, and Gly-27′ mimic the conserved hydrogen bonds observed with peptide analogue structures.[21,22] A conserved water−π interaction is observed between the P2′ aromatic ring of the inhibitor and the amide of Asp29′, which is similar to the interaction with darunavir and other structure-based designed PIs from our laboratories.[25,26] The bigger polar P1′ group of the 2-pyrrolidinone ring in inhibitor **19b** instead of the isobutyl group in PI's **1** and **2** introduces a new direct hydrogen bond with the backbone of HIV-1 protease and one new water-mediated hydrogen bond between the inhibitor and the side chain residue of the protease. The two alternative conformations of the P1′ group with occupancy of 0.5/0.5 provide more flexible binding within the S1′ subsite, which is likely to enhance the inhibition of resistant proteases.

As mentioned earlier, inhibitor **19b** maintained near full potency against multidrug-resistant clinical isolates examined. On the other hand, **19b** is less potent than darunavir possibly due to the bigger and less optimum size of the P1′-ligand. The design strategy of incorporating new polar interactions with conserved backbone regions of the protease warrants further investigation in light of the current molecular insight into these ligand-binding site interactions.

Conclusion

We have designed a number of HIV-1 protease inhibitors with methyl-2-pyrrolidinone and methyloxazolidinone as the P1′-ligand to enhance hydrogen bonding with the protein backbone atoms in the S1′-subsite. The ligands were synthesized in enantiomerically pure forms, and a series of inhibitors were prepared and evaluated in combination with P2-bis-THF and P2-Cp-THF ligands. In general, these inhibitors exhibited enzyme inhibitory activity lower than the corresponding inhibitors with a P1′-isobutyl group. Our SAR studies indicated the importance of ligand stereochemistry and also preference for the P2-Cp-THF ligand. Interestingly, the polar P1′-ligand influenced their cellular properties. The inhibitors exhibited reduction in antiviral activity possibly due to changes in the molecule's overall lipophilicity. Our investigation resulted in the identification of inhibitor **19b** which has displayed similar antiviral potency as the other FDA approved inhibitors such as indinavir, lopinavir, and amprenavir. Inhibitor **19b**, however, is nearly 10-fold less potent than darunavir. Of particular importance, **19b** has maintained full potency against the examined panel of multidrug-resistant HIV-1 variants. A high resolution X-ray structure of **19b**-bound HIV-1 protease revealed a new hydrogen bonding of the P1′-pyrrolidinone NH with the backbone carbonyl of Gly27′. Also, there is a water mediated hydrogen bond with the pyrrolidinone carboxyl and Arg8′ side chain. Furthermore, the P1′-pyrrolidinone showed two alternative conformations that filled the S1′ subsite. These new interactions and the conformational flexibility most likely contributed to its impressive properties against multidrug-resistant clinical variants. Further investigations including optimization of ligand-binding properties are in progress.

Experimental Section

General. All moisture sensitive reactions were carried out under nitrogen or argon atmosphere. Anhydrous solvents were obtained as follows: THF, diethyl ether, and benzene, distilled from sodium and benzophenone; dichloromethane, pyridine, triethylamine, and diisopropylethylamine, distilled from CaH_2. All other solvents were HPLC grade. Silica gel column chromatography was performed with Whatman 240−400 mesh silica gel under low pressure. TLC was carried out with E. Merck silica gel 60-F-254 plates. ^{1}H and ^{13}C NMR spectra were recorded on Varian Mercury 300 and Bruker Avance 400 and 500 spectrometers. Optical rotations were measured using a Perkin-Elmer 341 polarimeter.

(*S*)-5-(Aminomethyl)-2-pyrrolidinone 6. To a stirred solution of (*S*)-5-(hydroxymethyl)-2-pyrrolidinone **4** (300 mg, 2.61 mmol) and *p*-toluenesulfonyl chloride (646 mg, 3.34 mmol) in CH_2Cl_2 (6 mL) at 0 °C was added DMAP (64 mg, 0.52 mmol) and Et_3N (472 μL, 3.34 mmol). The resulting mixture was allowed to warm to 23 °C and stirred for 12 h. The reaction was then quenched with 7 mL of water, and the aqueous layer was extracted with CH_2Cl_2. The combined organic extracts were washed with 1 N HCl and dried over anhydrous Na_2SO_4. Removal of solvent under reduced pressure followed by flash chromatography purification (100% EtOAc as the eluent) yielded (*S*)-toluenesulfonate **5** ((0.7 g, 93%) as a yellowish solid. R_f = 0.50 (5% MeOH in $CHCl_3$); ^{1}H NMR (400 MHz, $CDCl_3$) δ 1.75−1.80 (m, 1H), 2.19−2.35 (m, 3H), 2.44 (s, 3H), 3.85−3.92 (m, 2H), 4.00−4.03 (m, 1H), 6.49 (s, 1H), 7.35 (d, 2H, J = 8.0 Hz), 7.77 (d, 2H, J = 8.1 Hz); ^{13}C NMR (100 MHz, $CDCl_3$) δ 21.6, 22.7, 29.2, 52.5, 71.9, 121.9, 130.0, 132.3, 145.3, 178.2.

To a stirred solution of the above tosylate (638 mg, 2.37 mmol) in DMF (20 mL) was added NaN_3 (462 mg, 2.37 mmol). The resulting solution was stirred at 55 °C for 9 h. Removal of solvent under reduced pressure followed by flash chromatography purification (6% MeOH in $CHCl_3$ as the eluent) provided the (*S*)-azidopyrrolidinone (330 mg, 99%) as a yellow oil. R_f = 0.50 (10% MeOH in $CHCl_3$); ^{1}H NMR (400 MHz, $CDCl_3$) δ 1.76−1.84 (m, 1H), 2.18−2.44 (m, 3H), 3.28 (dd, 1H, J = 6.5, 12.2 Hz), 3.43 (dd, 1H, J = 4.6, 12.3 Hz), 3.77−3.83 (m, 1H), 7.38 (s, 1H); ^{13}C NMR (100 MHz, $CDCl_3$) δ 23.9, 29.7, 53.6, 55.8, 178.7.

To a solution of the above azide (125 mg, 0.89 mmol) in EtOAc (10 mL) was added Pd/C (15 mg). The mixture was stirred at 23 °C under a hydrogen filled balloon for 4 h, then filtered over Celite, and the filter cake was washed with EtOAc and MeOH. Removal of solvent under reduced pressure followed by flash chromatography purification (5% MeOH in $CHCl_3$ as the eluent) afforded the corresponding (*S*)-amine **6** (105 mg, quantitive) as a yellow oil. R_f = 0.05 (20% MeOH in $CHCl_3$); ^{1}H NMR (400 MHz, $CDCl_3$) δ 1.41 (brs 2H), 1.56−1.65 (m, 1H), 2.01−2.12 (m, 1H), 2.19−2.24 (m, 2H), 2.52 (dd, 1H, J = 7.5, 12.8 Hz), 2.69 (dd, 1H, J = 4.3, 12.9 Hz), 3.50−3.57 (m, 1H), 7.90 (brs, 1H); ^{13}C NMR (100 MHz, $CDCl_3$) δ 24.0, 30.2, 47.3, 57.1, 179.0.

***tert*-Butyl-(2*R*,3*R*)-3-hydroxy-4-[((*S*)-5-oxopyrrolidin-2-yl)-methylamino]-1-phenylbutan-2-yl-carbamate 8.** To a solution of amine **6** (107 mg, 0.94 mmol) in *i*-PrOH (5 mL) were added *tert*-butyl-[*S*-(*R*,*R*)]-(-)-(1-oxiranyl-2-phenylethyl)carbamate **7** (62 mg, 0.23 mmol) and DIPEA (204 μL, 1.2 mmol). The resultant mixture was stirred at 65 °C for 18 h and then concentrated under reduced pressure. Flash chromatography purification (15% MeOH in $CHCl_3$ as the eluent) yielded title compound **8** (76 mg, 85%). R_f = 0.47 (25% MeOH in $CHCl_3$); ^{1}H NMR (400 MHz, $CDCl_3$) δ 1.30 (s, 9H), 1.62−1.71 (m, 1H), 2.13−2.18 (m, 1H), 2.30−2.32 (m, 2 H), 2.52 (d, 1H, J = 8.86 Hz), 2.64−2.73 (m, 4H), 2.96 (d, 1H, J = 9.8 Hz), 3.54 (s, 1H), 3.72−3.75 (m, 4H), 4.99 (brs, 1H), 7.15−7.26 (m, 5H), 8.02 (s, 1H); ^{13}C NMR (100 MHz, $CDCl_3$) δ 24.6, 28.3, 30.2, 36.3, 51.7, 54.0, 54.4, 55.3, 71.5, 79.2, 126.2, 128.2, 129.4, 138.1, 155.9, 178.9; LRMS-ESI (m/z) $[M + Na]^+$ 400.

***tert*-Butyl-(2*R*,3*R*)-3-hydroxy-4-(4-methoxy-*N*-(((*S*)-5-oxopyrrolidin-2-yl)methyl)phenylsulfonamido)-1-phenylbutan-2-ylcarbamate 9.** To a stirred solution of amine **8** (22 mg, 0.06 mmol) in CH_2Cl_2 (3 mL) and aqueous saturated $NaHCO_3$ (3 mL) was added 4-methoxybenzenesulfonyl chloride (35.6 mg, 0.17 mmol). This reaction mixture was stirred for 12 h followed by extraction of the aqueous layer with CH_2Cl_2; the combined organic extracts were dried over anhydrous Na_2SO_4. Removal of solvent under reduced pressure followed by flash chromatography purification (6% MeOH in $CHCl_3$ as the eluent) provided compound **9** (31 mg, quantitative). R_f = 0.40 (10% MeOH in $CHCl_3$); ^{1}H NMR (500 MHz, $CDCl_3$) δ 1.28 (s, 9H), 1.54−1.62 (m, 1H), 2.14−2.21 (m, 1H), 2.32−2.35 (m, 2H), 2.68−2.75 (m, 2H), 2.72 (s, 3H), 2.81−2.88 (m, 2H), 2.97−3.03 (m, 3H), 3.64−3.72 (m, 1H), 4.01−4.05 (m, 1H), 5.06 (d, 1H, J = 8.9 Hz), 6.93 (d, 2H, J = 8.6 Hz), 7.16−7.19 (m, 3H), 7.27−7.28 (m, 3H), 7.61 (d, 2H, J = 8.5 Hz); ^{13}C NMR (125 MHz, $CDCl_3$) δ 23.9, 28.1, 29.6, 29.9, 36.1, 53.4, 53.9, 54.5, 55.5, 56.0, 71.9, 79.5, 114.3, 126.3, 126.3, 129.3, 129.5, 137.7, 155.9, 163.1, 178.4; LRMS-ESI (*m/z*) [M + Na]$^+$ 570.

***tert*-Butyl-(2*R*,3*R*)-4-(4-Cbz-amino-*N*-(((*S*)-5-oxopyrrolidin-2-yl)methyl)phenylsulfonamido)-3-hydroxy-1-phenylbutan-2-ylcarbamate 10.** To a stirred solution of amine **8** (93.6 mg, 0.25 mmol) in CH_2Cl_2 (10 mL) and aqueous saturated $NaHCO_3$ (10 mL) was added 4-nitrobenzenesulfonyl chloride (60 mg, 0.27 mmol). This reaction mixture was stirred for 7 h followed by extraction of the aqueous layer with CH_2Cl_2; the combined organic extracts were dried over anhydrous Na_2SO_4. Removal of solvent under reduced pressure followed by flash chromatography purification (dry transfer, 8% MeOH in $CHCl_3$ as the eluent) provided (*S*)-nitrosulfonamide (112 mg, 80%) as a yellowish solid. R_f = 0.56 (10% MeOH in $CHCl_3$).

The above nitrosulfone (103 mg, 0.18 mmol) was dissolved in EtOAc (20 mL), and Pd/C (11 mg) was added. The mixture was stirred under a hydrogen filled balloon for 8 h at 23 °C. It was then filtered over Celite, and the filter cake was washed with EtOAc and MeOH. Removal of solvent under reduced pressure followed by flash chromatography purification (2.5% MeOH in $CHCl_3$ as the eluent) afforded the corresponding (*S*)-amine (77 mg, 79%) as a white solid. R_f = 0.26 (5% MeOH in $CHCl_3$); ^{1}H NMR (500 MHz, $CDCl_3$) 1.35 (s, 9H), 1.59−1.57 (m, 1H), 2.15−2.23 (m, 1H), 2.29−2.42 (m, 2H), 2.82−2.87 (m, 3H), 3.02 (dd, 1H, J = 4.75, 14.0), 3.13 (dd, 1H, J = 10, 13.2 Hz), 3.30 (dd, 2H, J = 1.8, 14.4 Hz), 3.73−3.82 (m, 1H), 3.90−3.95 (m, 1H), 3.99 (d, 1H, J = 6.2 Hz), 4.72 (d, 1H, J = 8.2 Hz), 6.72 (d, 2H, J = 7.9 Hz), 7.20−7.32 (m, 5H), 7.37 (s, 1H), 7.57 (d, 2H, J = 8.2 Hz); ^{13}C NMR (125 MHz, $CDCl_3$) δ 24.3, 28.6, 30.0, 36.5, 53.6, 54.4, 54.9, 56.6, 72.6, 79.8, 114.4, 125.0, 126.7, 128.7, 129.9, 130.0, 138.3, 151.5.

To a stirred solution of the above amine (33.1 mg, 0.06 mmol) in CH_2Cl_2 (3 mL) was added pyridine (30 μL, 0.37 mmol) and benzyl chloroformate (20 μL, 0.137 mmol). This reaction mixture was stirred for 3 h, then quenched with 5 drops of benzylamine followed by removal of solvent under reduced pressure. Column chromatography over silica gel (2.5% MeOH in $CHCl_3$ as the eluent) provided (*S*)-Cbz-amine **10** (41 mg, 99%) as a white solid. R_f = 0.37 (5% MeOH in $CHCl_3$); ^{1}H NMR (500 MHz, $CDCl_3$) δ 1.56 (brs, 1H), 2.12−2.18 (m, 1H), 2.26−2.41 (m, 2H), 2.71−2.78 (m, 2H), 2.79−89 (m, 1H), 3.02 (dd, 1H, J = 8.2, 18.0 Hz), 3.19−3.26 (m, 1H), 3.38 (d, 1H, J = 14.4 Hz), 3.77 (brs, 1H), 3.94−3.99 (m, 2H), 4.73 (d, 1H, J = 8.5 Hz), 5.21 (s, 2H), 7.19−7.22 (m, 3H), 7.25−7.29 (m, 3H), 7.31−7.39 (m, 4H), 7.57 (d, 2H, J = 7.6 Hz), 7.69 (d, 2H, J = 7.7 Hz); ^{13}C NMR (125 MHz, $CDCl_3$) δ 24.1, 28.7, 30.1, 36.6, 53.3, 54.3, 54.8, 56.8, 67.7, 72.6, 80.0, 118.6, 126.8, 128.7, 128.8, 128.9, 129.0, 129.4, 129.9, 131.6, 136.0, 138.1, 143.0, 153.3, 156.3, 178.9; LRMS-ESI (*m/z*) [M + Na]$^+$ 689.

***tert*-Butyl-(2*R*,3*R*)-3-hydroxy-4-(4-methoxy-*N*-(((*R*)-5-oxopyrrolidin-2-yl)methyl)phenylsulfonamido)-1-phenylbutan-2-ylcarbamate 11.** To a stirred solution of (*R*)-5-(hydroxymethyl)-2-pyrrolidinone *ent*-**5** (500 mg, 4.34 mmol) and *p*-toluenesulfonyl chloride (1.08 g, 5.6 mmol) in CH_2Cl_2 (10 mL) at 0 °C were added DMAP (106 mg, 0.87 mmol) and Et_3N (780 μL, 5.6 mmol). The resulting mixture was allowed to warm to 23 °C and stirred for 12 h. The reaction was then quenched with 10 mL of water, and the aqueous layer was extracted with CH_2Cl_2. The combined organic extracts were washed with 1 N HCl and dried over anhydrous Na_2SO_4. Removal of solvent under reduced pressure followed by flash chromatography (2.5% MeOH in $CHCl_3$ as the eluent) yielded the (*R*)-toluenesulfonate (1.8 g, 93%) as a yellowish solid. R_f = 0.50 (5% MeOH in $CHCl_3$); ^{1}H NMR (400 MHz, $CDCl_3$) δ 1.70−1.79 (m, 1H), 2.13−2.35 (m, 3H), 2.42 (s, 3H), 3.84−3.89 (m, 2H), 3.96−3.04 (m, 1H), 6.76 (s, 1H), 7.33 (d, 2H, J = 8.04 Hz), 7.76 (d, 2H, J = 8.2 Hz); ^{13}C NMR (100 MHz, $CDCl_3$) δ 21.6, 22.7, 29.3, 52.6, 71.9, 127.9, 130.0, 132.3, 145.3, 178.1.

To a stirred solution of the above toluenesulfonate (1.08 g, 4.03 mmol) in DMF (30 mL) was added NaN_3 (1.31 g, 20.2 mmol). The resulting solution was stirred at 55 °C for 12 h. Solvent was then removed under reduced pressure followed by flash chromatography purification (6% MeOH in $CHCl_3$ as the eluent), providing the (*R*)-azidopyrrolidinone (558 mg, 99%) as a yellow oil. R_f = 0.44 (5% MeOH in $CHCl_3$); ^{1}H NMR (500 MHz, $CDCl_3$) δ 1.72−1.79 (m, 1H), 2.13−2.37 (m, 3H), 3.22 (dd, 1H, J = 6.3, 12.3 Hz), 3.37 (dd, 1H, J = 4.7, 12.3 Hz), 3.72−3.78 (m, 1H), 7.69 (s, 1H); ^{13}C NMR (125 MHz, $CDCl_3$) δ 24.3, 30.2, 54.1, 56.1, 179.3.

To a solution of the above azide (528 mg, 3.77 mmol) in EtOAc (35 mL) was added Pd/C (40 mg). The mixture was stirred at 23 °C under a hydrogen filled balloon for 4 h, then filtered over Celite, and the filter cake was washed with EtOAc and MeOH. Removal of solvent under reduced pressure followed by flash chromatography purification (5% MeOH in $CHCl_3$ as the eluent) afforded the (*R*)-amine *ent*-**6** (257 mg, 95%) as a yellow oil. R_f = 0.05 (20% MeOH in $CHCl_3$); ^{1}H NMR (400 MHz, $CDCl_3$) δ 1.59−1.69 (m, 1H), 2.06−2.15 (m, 1H), 2.23−2.30 (m, 4H), 2.57 (dd, 1H, J = 7.6, 12.8 Hz), 2.74 (dd, 1H, J = 4.1, 12.9 Hz), 3.56−3.65 (m, 1H), 7.80 (brs, 1H); ^{13}C NMR (100 MHz, $CDCl_3$) δ 24.1, 30.2, 47.1, 56.8, 179.0.

To a solution of amine *ent*-**6** (430 mg, 3.76 mmol) in *i*-PrOH (20 mL) were added *tert*-butyl-[*S*-(*R*,*R*)]-(−)-(1-oxiranyl-2-phenylethyl)carbamate **7** (250 mg, 0.94 mmol) and *i*-Pr_2EtN (1.5 mL, 8.6 mmol). The resultant mixture was stirred at 65 °C for 36 h and then concentrated under reduced pressure. Flash chromatography purification (10% MeOH in $CHCl_3$ as the eluent) yielded the (*R*)-hydroxylamine (**8***R*) (300 mg, 84%). R_f = 0.33 (20% MeOH in $CHCl_3$); ^{1}H NMR (400 MHz, $CDCl_3$) δ 1.33 (s, 9H), 1.64−1.73 (m, 1H), 2.13−2.22 (m, 1H), 2.28−2.34 (m, 2 H), 2.54 (dd, 1H, J = 9.0, 11.8 Hz), 2.65 (dd, 1H, J = 7.2, 13.2 Hz), 2.73−2.85 (m, 4H), 2.94 (dd, 1H, J = 4.4, 14.0 Hz), 3.43 (s, 1H), 3.51−3.60 (m, 1H), 3.70−3.76 (m, 1H), 3.79−3.84 (m, 1H), 5.02 (d, 1H, J = 8.9 Hz), 7.16−7.27 (m, 5H), 7.94 (s, 1H); ^{13}C NMR (100 MHz, $CDCl_3$) δ 24.6, 28.3, 30.2, 36.3, 52.1, 54.2, 54.6, 55.4, 71.6, 79.2, 126.2, 128.3, 129.4, 138.1, 155.9, 178.9; LRMS-ESI (*m/z*) [M + Na]$^+$ 400.

To a stirred solution of above (*R*)-hydroxylamine (**8***R*) (40 mg, 0.105 mmol) in CH_2Cl_2 (4 mL) and aqueous saturated $NaHCO_3$ (4 mL) was added 4-methoxybenzenesulfonyl chloride (66 mg, 0.318 mmol). This reaction mixture was stirred for 12 h followed by extraction of the aqueous layer with CH_2Cl_2; the combined organic extracts were dried over anhydrous Na_2SO_4. Removal of solvent under reduced pressure followed by flash chromatography purification (4% MeOH in $CHCl_3$ as the eluent) provided compound **11** (54 mg, 93%). R_f = 0.40 (10% MeOH in $CHCl_3$); ^{1}H NMR (400 MHz, $CDCl_3$) δ 1.32 (s, 9H), 1.64−1.68 (m, 1H), 2.17−2.21 (m, 2H), 2.34−2.40 (m, 2H), 2.76−2.84 (m, 1H), 2.91−3.06 (m, 3H), 3.16−3.29 (m, 2H), 3.75−3.80 (m, 1H), 3.84 (s, 3H), 3.96−4.02 (m, 2H), 4.99 (d, 1H, J = 8.7 Hz), 6.95 (d, 2H, J = 8.8 Hz), 7.16−7.28 (m, 5H), 7.68 (d, 2H, J = 8.8 Hz), 7.93 (s, 1H); ^{13}C NMR (100 MHz, $CDCl_3$) δ 24.4, 28.2, 29.9, 35.7, 35.4, 54.7, 55.2, 55.6, 55.8, 57.8, 73.9, 79.5, 114.4, 126.2, 128.3, 129.3, 129.5, 138.0, 155.9, 163.1, 178.6; LRMS-ESI (*m/z*) [M + Na]$^+$ 670.

tert*-Butyl-(2*R*,3*R*)-4-(4-Cbz-amino-*N*-(((*R*)-5-oxopyrrolidin-2-yl)methyl)phenylsulfonamido)-3-hydroxy-1-phenylbutan-2-ylcarbamate 12.** To a stirred solution of (*R*)-hydroxylamine (**8R*) (116 mg, 0.3 mmol) in CH_2Cl_2 (10 mL) and aqueous saturated $NaHCO_3$ (10 mL) was added 4-nitrobenzenesulfonyl chloride (74 mg, 0.33 mmol). This reaction mixture was stirred for 12 h followed by extraction of the aqueous layer with CH_2Cl_2; the combined organic extracts were dried over anhydrous Na_2SO_4. Removal of solvent under reduced pressure followed by flash chromatography purification (dry transfer, 5% MeOH in $CHCl_3$ as the eluent) provided the (*R*)-nitrosulfonamide (164 mg, 96%) as a yellowish solid. R_f = 0.56 (10% MeOH in $CHCl_3$).

The above nitrosulfonamide (154 mg, 0.27 mmol) was redisolved in EtOAc (25 mL) and treated with Pd/C (16 mg) under argon. Argon was then replaced with a hydrogen filled balloon, and the mixture was allowed to stir for 12 h at 23 °C. It was then filtered over Celite, and the filter cake was washed with EtOAc and MeOH. Removal of solvent under reduced pressure followed by flash chromatography purification (6% MeOH in $CHCl_3$ as the eluent) afforded the corresponding (*R*)-aniline (123 mg, 83%) as an amorphous solid. R_f = 0.45 (10% MeOH in $CHCl_3$); ^1H NMR (500 MHz, $CDCl_3$) δ 1.31 (s, 9H), 1.58−1.64 (m, 1H), 2.15−2.21 (m, 1H), 2.29 (t, 2H, J = 8.2 Hz), 2.73−2.86 (m, 3H), 2.99 (dd, 1H, J = 4.4, 13.9 Hz), 3.23 (d, 1H, J = 13.8 Hz), 3.30 (d, 1H, J = 14.8 Hz), 3.74 (brs, 1H), 3.92 (brs, 1H), 3.99 (d, 1H, J = 5.7), 4.31 (s, 1H), 5.01 (d, 1H, J = 9.1 Hz), 6.63 (d, 2H, J = 8.5 Hz), 7.16−7.21 (m, 3H), 7.24−7.27 (m, 2H), 7.48 (d, 2H, J = 8.5 Hz); ^{13}C NMR (125 MHz, $CDCl_3$) δ 24.3, 28.1, 29.8, 35.5, 54.6, 55.0, 55.5, 57.7, 73.8, 79.5, 113.9, 125.0, 126.2, 128.2, 129.3, 129.4, 137.8, 151.0, 155.9, 178.2; LRMS-ESI (m/z) $[M + Na]^+$ 555.

To a stirred solution of the above (*R*)-aniline (101 mg, 0.19 mmol) in CH_2Cl_2 (15 mL) was added pyridine (34 μL, 0.41 mmol) and benzyl chloroformate (60 μL, 0.41 mmol). This reaction mixture was stirred for 1.5 h, then quenched with 3 drops of benzylamine, followed by removal of solvent under reduced pressure. Column chromatography over silica gel (6% MeOH in $CHCl_3$ as the eluent) provided the (*R*)-Cbz-amine **12** (120 mg, 95%) as a white solid. R_f = 0.35 (10% MeOH in $CHCl_3$); ^1H NMR (500 MHz, $CDCl_3$) δ 1.29 (s, 9H), 1.55−1.65 (m, 1H), 2.15−2.23 (m, 1H), 2.26−2.31 (m, 2H), 2.60−2.75 (m, 3H), 2.97 (dd, 1H, J = 8.2, 18.1 Hz), 3.29 (d, 1H, J = 17.7 Hz), 3.36 (dd, 1H, J = 2.4, 14.9 Hz), 3.64 (s, 1H), 3.88−3.92 (m, 1H), 3.98−4.02 (m, 1H), 5.12 (d, 1H, J = 9.0 Hz), 5.17 (s, 2H), 7.14−7.19 (m, 3H), 7.21−7.28 (m, 3H), 7.30−7.37 (m, 4H), 7.54 (d, 2H, J = 8.6 Hz), 7.63 (d, 2H, J = 8.8); ^{13}C NMR (125 MHz, $CDCl_3$) δ 24.8, 28.6, 30.2, 36.0, 55.1, 55.8, 55.9, 58.2, 67.6, 74.4, 80.0, 118.6, 126.7, 128.6, 128.7, 128.8, 129.0, 129.0, 129.7, 130.3, 131.2, 136.1, 138.2, 143.4, 153.6, 178.9; LRMS-ESI (m/z) $[M + Na]^+$ 689.

(3*R*,3a*S*,6a*R*)-Hexahydrofuro[2,3-*b*]furan-3-yl(2*S*,3*R*)-3-hydroxy-4-(4-methoxy-*N*-(((*S*)-5-oxopyrrolidin-2-yl)methyl)phenylsulfonamido)-1-phenylbutan-2-ylcarbamate 17a. A solution of compound **9** (10 mg, 0.02 mmol) in 30% trifluoroacetic acid (in CH_2Cl_2, 3 mL) was stirred 23 °C for 40 min, then concentrated under reduced pressure to give the crude amine **13***S*. This residue was redissolved in CH_2Cl_2 (3 mL), treated with Et_3N (20 μL, 0.13 mmol), followed by carbonate **15** (5.5 mg, 0.02 mmol) and stirred at 23 °C for 12 h. The reaction mixture was then concentrated under reduced pressure, and the residue was purified by flash chromatography (2% MeOH in $CHCl_3$ as the eluent) to give inhibitor **17a** (11.3 mg, 98%) as a white solid. R_f = 0.48 (10% MeOH in $CHCl_3$); ^1H NMR (500 MHz, $CDCl_3$) δ 1.48 (dd, 1H, J = 5.5, 13.2 Hz), 1.58−1.68 (m, 2H), 2.17−2.26 (m, 1H), 2.34−2.49 (m, 2H), 2.76 (dd, 1H, J = 9.8, 14.0 Hz), 2.85−2.95 (m, 3H), 3.10−3.16 (m, 2H), 3.22 (dd, 1H, (dd, 1H, J = 9.9, 13.7 Hz), 3.67−3.74 (m, 2H), 3.82−3.85 (dt, 1H, J = 1.8, 8.4 Hz), 3.87 (s, 3H), 3.94 (dd, 1H, J = 6.2, 9.6 Hz), 3.96−4.01 (m, 1H), 4.04−4.08 (m, 1H), 5.0 (q, 1H, J = 6.1, 7.9 Hz), 5.64 (d, 1H, J = 5.2 Hz), 6.98 (d, 2H, J = 8.9 Hz), 7.19−7.29 (m, 3H), 7.26−7.29 (m, 2H), 7.58 (brs, 1H), 7.69 (d, 2H, J = 8.8 Hz); ^{13}C NMR (125 MHz, $CDCl_3$) δ 23.9, 25.7, 29.5, 35.9, 45.2, 53.4, 53.9, 55.1, 55.6, 56.4, 69.5, 70.8, 72.3, 73.3, 109.2, 114.4, 126.4, 128.3, 128.6, 129.2, 129.4, 137.6, 155.4, 163.2, 178.5. LRMS-ESI (m/z) $[M + H]^+$ 604.2; HRMS-ESI (m/z) $[M + H]^+$ calcd for $C_{29}H_{38}N_3O_9S$ 604.2329, found 604.2332.

(3a*S*,5*R*,6a*R*)-Hexahydro-2*H*-cyclopenta[*b*]furan-5-yl-(2*S*,3*R*)-3-hydroxy-4-(4-methoxy-*N*-(((*S*)-5-oxopyrrolidin-2-yl)methyl)phenylsulfonamido)-1-phenylbutan-2-ylcarbamate 17b. A solution of compound **9** (11.8 mg, 0.02 mmol) in 30% trifluoroacetic acid (in CH_2Cl_2, 1.5 mL) was stirred at 23 °C for 40 min, then concentrated under reduced pressure to give the crude amine **13***S*. This crude residue was redissolved in CH_2Cl_2 (1.5 mL), treated with Et_3N (63 μL, 0.45 mmol), followed by carbonate **16** (6.4 mg, 0.02 mmol), and stirred at 23 °C for 6 h. The reaction mixture was then concentrated under reduced pressure and the residue was purified by flash chromatography (1% MeOH in $CHCl_3$ as the eluent) to give inhibitor **17b** (11.5 mg, 87%) as a white solid. R_f = 0.35 (5% MeOH in $CHCl_3$); ^1H NMR (500 MHz, $CDCl_3$) δ 1.45 (d, 1H, J = 14.3 Hz), 1.55−1.59 (m, 1H), 1.88 (d, 1H, J = 15.1 Hz), 1.95−2.06 (m, 3H), 2.17−2.24 (m, 1H), 2.33−2.48 (m, 2H), 2.60−2.67 (m, 1H), 2.78 (dd, 1H, J = 9.1, 14.1 Hz), 2.88−2.97 (m, 2H), 3.09 (dd, 1H, J = 4.3, 14.1 Hz), 3.12−3.18 (m, 2H), 3.64−3.68 (m, 1H), 3.82−3.85 (m, 2H), 3.86 (s, 3H), 3.89−3.95 (m, 1H), 3.99−4.05 (m, 1H), 4.39−4.42 (m, 1H), 4.69 (d, 1H, J = 4.1 Hz), 4.87−4.90 (m, 1H), 4.91 (d, 1H, J = 8.9 Hz), 6.98 (d, 2H, J = 8.9 Hz), 7.20−7.23 (m, 3H), 7.27−7.30 (m, 2H), 7.42 (s, 1H), 7.70 (d, 2H, J = 8.9 Hz); ^{13}C NMR (125 MHz, $CDCl_3$) δ 24.0, 29.8, 33.8, 35.9, 38.3, 39.4, 41.5, 53.2, 53.3, 53.9, 54.8, 55.5, 56.3, 67.6, 72.2, 83.7, 114.3, 126.4, 128.4, 128.7, 129.3, 129.5, 137.5, 156.1, 163.1, 178.3. LRMS-ESI (m/z) $[M + Na]^+$ 624.0; HRMS-ESI (m/z) $[M + Na]^+$ calcd for $C_{30}H_{39}N_3NaO_8S$ 624.2356, found 624.2352.

(3*R*,3a*S*,6a*R*)-Hexahydrofuro[2,3-*b*]furan-3-yl(2*S*,3*R*)-4-(4-amino-*N*-(((*S*)-5-oxopyrrolidin-2-yl)methyl)phenylsulfonamido)-3-hydroxy-1-phenylbutan-2-ylcarbamate 18a. The Cbz-protected amine **10** (31 mg, 0.04 mmol) was treated with 30% trifluoroacetic acid in CH_2Cl_2 (6 mL) and stirred at 23 °C for 40 min, then concentrated under reduced pressure to give the crude amine **14***S*. This residue was redissolved in CH_2Cl_2 (6 mL), charged with Et_3N (64 μL, 0.46 mmol), followed by carbonate **15** (14 mg, 0.05 mmol), and stirred at 23 °C for 12 h. Reaction was quenched with 3 drops of benzylamine and concentrated under reduced pressure. Flash chromatography purification (4% MeOH in $CHCl_3$ as the eluent) provided the Cbz-protected inhibitor (23 mg, 86%) as a white solid. R_f = 0.46 (10% MeOH in $CHCl_3$).

To the above Cbz-protected inhibitor (13.3 mg, 0.018 mmol), in EtOAc (6 mL) under argon, was added Pd/C (3 mg). The mixture was stirred at 23 °C under a hydrogen filled balloon for 3 h, then filtered over Celite, and the filter cake was washed with EtOAc and MeOH. Removal of solvent under reduced pressure followed by flash chromatography purification (3% MeOH in $CHCl_3$ as the eluent) provided the title inhibitor **18a** (7.4 mg, 68%) as a white solid. R_f = 0.19 (5% MeOH in $CHCl_3$); ^1H NMR (500 MHz, $CDCl_3$) δ 1.44 (d, 1H, J = 5.4 Hz), 1.59−1.69 (m, 2H), 2.16−2.25 (m, 1H), 2.36 (t, 2H, J = 7.9 Hz), 2.68 (dd, 1H, J = 9.8, 13.9 Hz), 2.85−2.95 (m, 3H), 3.03−3.09 (m, 2H), 3.13 (dd, 1H, J = 4.4, 14.1 Hz), 3.67−3.72 (m, 2H), 3.79−3.89 (m, 3H), 3.93 (dd, 1H, J = 6.0, 9.7 Hz), 4.01−4.06 (m, 1H), 4.96 (q, 1H, J = 5.9, 7.9 Hz), 5.63 (d, 1H, J = 5.1 Hz), 6.72 (d, 2H, J = 8.2 Hz), 7.17−7.21 (m, 3H), 7.24−7.28 (m, 2H), 7.50 (d, 2H, J = 8.4 Hz); ^{13}C NMR (125 MHz, $CDCl_3$) δ 24.3, 26.2, 30.0, 36.6, 45.8, 53.6, 54.2, 55.6, 56.6, 70.0, 71.5, 72.7, 73.6, 109.7, 114.6, 124.9, 126.8, 128.8, 129.7, 129.9, 130.3, 151.4, 155.9, 178.3. LRMS-ESI (m/z) $[M + H]^+$ 589.2; HRMS-ESI (m/z) $[M + H]^+$ calcd for $C_{28}H_{37}N_4O_8S$ 589.2332, found 589.2336.

(3a*S*,5*R*,6a*R*)-Hexahydro-2*H*-cyclopenta[*b*]furan-5-yl-(2*S*,3*R*)-4-(4-amino-*N*-(((*S*)-5-oxopyrrolidin-2-yl)methyl)phenylsulfonamido)-3-hydroxy-1-phenylbutan-2-ylcarbamate 18b. The Cbz-protected amine **10** (29.6 mg, 0.04 mmol) was treated with 30% trifluoroacetic acid (in CH_2Cl_2, 6 mL) and stirred at 23 °C for 40 min, then concentrated under reduced pressure to give the crude amine **14***S*. The residue was redissolved in CH_2Cl_2 (6 mL), charged with Et_3N (31 μL, 0.22 mmol), followed by carbonate **16** (13.1 mg, 0.05 mmol), and stirred at 23 °C for 4 h. Reaction was

quenched with 2 drops of benzylamine and concentrated under reduced pressure. Flash chromatography purification (4% MeOH in $CHCl_3$ as the eluent) provided the Cbz-protected inhibitor (26.1 mg, 82%) as a white solid. R_f = 0.49 (10% MeOH in $CHCl_3$).

To a solution of the above protected inhibitor (17 mg, 0.02 mmol), in EtOAc (5 mL) under argon, was added Pd/C (3 mg). The mixture was stirred at 23 °C under a H_2 filled balloon for 5 h, then filtered over Celite, and the filter cake was washed with EtOAc and MeOH. Removal of solvent under reduced pressure, followed by flash chromatography purification (5% MeOH in $CHCl_3$ as the eluent) provided inhibitor **18b** (14 mg, 75%) as a white solid. R_f = 0.27 (10% MeOH in $CHCl_3$); ^{1}H NMR (500 MHz, $CDCl_3$) δ 1.41−1.45 (m, 1H), 1.56−1.67 (m, 3H), 1.85 (d, 1H, J = 13.4 Hz), 1.96−2.04 (m, 3H), 2.14−2.21 (m, 1H), 2.31−2.42 (m, 2H), 2.61 (brs, 1H), 2.74−2.85 (m, 3H), 3.09 (dd, 1H, J = 4.4, 14.4 Hz), 3.15−3.20 (m, 1H), 3.25 (d,1H, J = 14.3 Hz), 3.66−3.70 (q, 1H, J = 7.1, 7.4 Hz), 3.83−3.88 (m, 2H), 3.91−3.96 (m, 1H), 3.96−4.25 (m, 1H), 4.40 (t, 1H, J = 5.9 Hz), 4.87 (brs, 1H), 4.93 (d, 1H, J = 8.9 Hz), 6.69 (d, 2H), 7.18−7.22 (m, 3H), 7.28−7.30 (m, 2H), 7.55 (d, 2H, J = 8.4 Hz), 7.63 (s, 1H); ^{13}C NMR (125 MHz, $CDCl_3$) δ 24.3, 30.1, 34.1, 36.7, 38.7, 39.8, 41.9, 53.5, 54.3, 55.3, 56.8, 68.0, 72.8, 84.1, 114.6, 125.3, 126.8, 128.8, 129.9, 130.1, 138.1, 151.4, 156.6, 178.9. LRMS-ESI (m/z) [M + H]$^+$ 586.9; HRMS-ESI (m/z) [M + H]$^+$ calcd for $C_{29}H_{39}N_4O_7S$ 587.2539, found 587.2539.

(3*R*,3a*S*,6a*R*)-Hexahydrofuro[2,3-*b*]furan-3-yl-(2*S*,3*R*)-3-hydroxy-4-(4-methoxy-*N*-(((*R*)-5-oxopyrrolidin-2-yl)methyl)phenylsulfonamido)-1-phenylbutan-2ylcarbamate 19a. A solution of compound **11** (20 mg, 0.03 mmol) in 30% trifluoroacetic acid (in CH_2Cl_2, 3 mL) was stirred 23 °C for 40 min, then concentrated under reduced pressure. The residue was redissolved in CH_2Cl_2 (3 mL), treated with Et_3N (51 μL, 0.36 mmol), followed by carbonate **15** (11 mg, 0.04 mmol), and stirred at 23 °C for 12 h. The reaction mixture was then concentrated under reduced pressure and the residue was purified by flash chromatography (2% MeOH in $CHCl_3$ as the eluent) to give inhibitor **19a** (21 mg, 92%) as a white solid. R_f = 0.41 (10% MeOH in $CHCl_3$); ^{1}H NMR (500 MHz, $CDCl_3$) δ 1.44 (dd, 1H, J = 5.6, 13.2 Hz), 1.57−1.67 (m, 2H), 1.81−1.91 (m, 1H), 2.19−2.27 (m, 1H), 2.33−2.41 (m, 2H), 2.73 (dd, 1H J = 10.35, 13.9 Hz), 2.83−2.91 (m, 2H), 2.95 (dd, 1H, J = 8.9, 14.9 Hz), 3.11 (dd, 1H, J = 4.2, 14.0 Hz), 3.26−3.30 (ddd, 2H, J = 2.6, 7.0, 14.3 Hz), 3.64−3.70 (m, 1H), 3.74 (dd, 1H, J = 5.5, 9.8 Hz), 3.76−3.81 (dt, 1H, J = 1.62, 8.0 Hz), 3.87 (s, 3H), 3.89−3.93 (q, 1H, J = 4.0, 5.6 Hz), 4.03−4.06 (m, 2H), 4.98−5.02 (q, 1H, J = 5.65, 7.9 Hz), 5.62 (d, 1H, J = 5.4 Hz), 6.98 (d, 2H, J = 8.9 Hz), 7.17−7.27 (m, 5H), 7.70 (d, 2H, J = 8.8 Hz), 7.89 (s, 1H); ^{13}C NMR (125 MHz, $CDCl_3$) δ 24.2, 25.7, 29.8, 35.4, 45.4, 55.0, 55.3, 55.5, 55.7, 58.1, 69.5, 71.0, 73.3, 74.0, 109.2, 114.4, 126.3, 128.3, 128.8, 129.2, 129.4, 137.8, 155.5, 163.2, 178.5. LRMS-ESI (m/z) [M + Na]$^+$ 626.3; HRMS-ESI (m/z) [M + Na]$^+$ calcd for $C_{29}H_{37}N_3$ Na O_9S 626.2148, found 626.2156.

(3a*S*,5*R*,6a*R*)-Hexahydro-2*H*-cyclopenta[*b*]furan-5-yl-(2*S*,3*R*)-3-hydroxy-4-(4-methoxy-*N*-(((*R*)-5-oxopyrrolidin-2-yl)methyl)phenylsulfonamido)-1-phenylbutan-2-ylcarbamate 19b. A solution of compound **11** (21 mg, 0.04 mmol) in 30% trifluoroacetic acid (in CH_2Cl_2, 3 mL) was stirred at 23 °C for 40 min, then concentrated under reduced pressure. The residue was redissolved in CH_2Cl_2 (3 mL), treated with Et_3N (27 μL, 0.19 mmol), followed by carbonate **16** (12 mg, 0.04 mmol), and stirred at 23 °C for 12 h. The reaction mixture was then concentrated under reduced pressure and the residue was purified by flash chromatography (1% MeOH in $CHCl_3$ as the eluent) to give inhibitor **19b** (21 mg, 93%) as a white solid. R_f = 0.31 (5% MeOH in $CHCl_3$); ^{1}H NMR (500 MHz, $CDCl_3$) δ 1.48 (d, 1H, J = 14.1 Hz), 1.58−1.62 (m, 1H), 1.83−2.04 (m, 5H), 2.19−2.25 (m, 1H), 2.31−2.41 (m, 2H), 2.59−2.67 (m, 1H), 2.73 (dd, 1H, J = 9.0, 13.9 Hz), 3.03 (dd, 1H, J = 7.0, 15.0 Hz), 3.08−3.16 (m, 2H), 3.19 (d, 1H, J = 14.9 Hz), 3.57−3.63 (m, 1H), 3.83−3.86 (m, 3H), 3.86 (s, 3H), 3.94−3.99 (m, 1H), 4.78 (d, 1H, J = 13.7 Hz), 4.90 (s, 1H), 5.36 (d, 1H, J = 8.1 Hz), 6.97 (d, 2H, J = 8.6 Hz), 7.18−7.28 (m, 5H), 7.46 (d, 1H, J = 18.4 Hz), 7.70 (d, 2H, J = 8.8 Hz); ^{13}C NMR (125 MHz, $CDCl_3$) δ 22.5, 30.0, 31.4, 33.9, 35.8, 38.2, 39.5, 41.7, 54.6, 54.9, 55.5, 56.0, 57.7, 67.7, 74.0, 83.9, 114.4, 126.2, 128.2, 128.9, 129.3, 129.4, 137.9, 156.1, 163.1, 178.5. LRMS-ESI (m/z) [M + H]$^+$ 601.7; HRMS-ESI (m/z) [M + H]$^+$ calcd for $C_{30}H_{40}N_3O_8S$ 602.2536, found 602.2536.

(3*R*,3a*S*,6a*R*)-Hexahydrofuro[2,3-*b*]furan-3-yl-(2*S*,3*R*)-4-(4-amino-*N*-(((*R*)-5-oxopyrrolidin-2-yl)methyl)phenylsulfonamido)-3-hydroxy-1-phenylbutan-2-ylcarbamate 20a. A solution of the (*R*)-aniline **12** (15 mg, 0.03 mmol) in 30% trifluoroacetic acid (in CH_2Cl_2, 3 mL) was stirred at 23 °C for 40 min, then concentrated under reduced pressure. The residue was redissolved in CH_2Cl_2 (3 mL), treated with Et_3N (40 μL, 0.28 mmol), followed by carbonate **15** (9.2 mg, 0.03 mmol), and stirred at 23 °C for 6 h. The reaction mixture was then concentrated under reduced pressure and the residue was purified by flash chromatography (4% MeOH in $CHCl_3$ as the eluent) to give inhibitor **20a** (12.5 mg, 75%) as a white solid. R_f = 0.26 (10% MeOH in $CHCl_3$); ^{1}H NMR (500 MHz, $CDCl_3$) δ 1.35 (dd, 1H, J = 5.7 Hz), 1.50−1.63 (m, 2H), 2.15−2.23 (m, 1H), 2.27−2.31 (m, 2H), 2.56−2.72 (m, 3H), 2.82−2.87 (m, 2H), 3.07 (dd, 1H, J = 4.0, 14.0 Hz), 3.36 (q, 1H, J = 1.4, 3.5 Hz), 3.36 (q, 1H, J = 2.0, 3.4 Hz), 3.60−3.65 (m, 1H), 3.70 (dd, 1H, J = 5.4, 9.8 Hz), 3.75−3.79 (dt, 1H, J = 1.96, 8.3 Hz), 3.80−3.86 (m, 1H), 3.88 (dd, 1H, J = 5.9, 9.8 Hz), 3.90−3.94 (m, 1H), 3.99−4.02 (m, 1H), 4.92−4.97 (q, 1H, J = 5.7, 8.1 Hz), 5.58 (d, 1H, J = 5.8 Hz), 5.92 (d, 1H, J = 9.5 Hz), 6.63 (d, 2H, J = 8.7 Hz), 7.13−7.22 (m, 5H), 7.46 (d, 2H, J = 8.7 Hz); ^{13}C NMR (125 MHz, $CDCl_3$) δ 24.1, 25.7, 29.7, 35.3, 45.4, 55.0, 55.5, 55.6, 58.1, 69.5, 71.0, 73.1, 73.9, 109.2, 113.8, 124.2, 126.2, 128.2, 129.1, 129.3, 137.8, 151.4, 155.6, 178.6. LRMS-ESI (m/z) [M + Na]$^+$ 611.4; HRMS-ESI (m/z) [M + Na]$^+$ calcd for $C_{28}H_{36}N_4NaO_8S$ 611.2152, found 611.2149.

(3a*S*,5*R*,6a*R*)-Hexahydro-2*H*-cyclopenta[*b*]furan-5-yl-(2*S*,3*R*)-4-(4-amino-*N*-(((*R*)-5-oxopyrrolidin-2-yl)methyl)phenylsulfonamido)-3-hydroxy-1-phenylbutan-2-ylcarbamate 20b. The Cbz-amine **12** (40 mg, 0.06 mmol) was treated with 30% trifluoroacetic acid (in CH_2Cl_2, 6 mL) and stirred at 23 °C for 40 min, then concentrated under reduced pressure. This residue was redissolved in CH_2Cl_2 (6 mL), charged with Et_3N (42 μL, 0.3 mmol), followed by carbonate **16** (19 mg, 0.07 mmol), and stirred at 23 °C for 12 h. Reaction was quenched with 3 drops of benzylamine and concentrated under reduced pressure. Flash chromatography purification (5% MeOH in $CHCl_3$ as the eluent) provided the Cbz-protected inhibitor (32.1 mg, 75%) as a white solid. R_f = 0.41 (10% MeOH in $CHCl_3$).

To the above Cbz-protected inhibitor (25.8 mg, 0.03 mmol), in EtOAc (5 mL) under argon, was added Pd/C (5 mg). The mixture was stirred at 23 °C under a hydrogen filled balloon for 3 h, then filtered over Celite, and the filter cake was washed with EtOAc and MeOH. Removal of solvent under reduced pressure followed by flash chromatography purification (7.5% MeOH in $CHCl_3$ as the eluent) provided the title inhibitor **20b** (16.2 mg, 77%) as a white solid. R_f = 0.51 (15% MeOH in $CHCl_3$); ^{1}H NMR (500 MHz, $CDCl_3$) δ 1.46 (m, 1H), 1.58−1.64 (m, 1H), 1.77−1.84 (m, 1H), 1.86−2.04 (m, 5H), 2.15−2.23 (m, 1H), 2.32−2.36 (m, 2H), 2.59−2.65 (m, 1H), 2.68 (dd, 1H, J = 9.2, 14.0 Hz), 2.95−3.04 (m, 2H), 3.11 (d, 2H, J = 13.7 Hz), 3.18 (d, 1H, J = 14.9 Hz), 3.57−3.62 (q, 1H, J = 6.9, 7.7 Hz), 3.82−3.87 (q, 2H, J = 6.5, 7.9 Hz), 3.92−3.97 (m, 1H), 4.30 (s, 2H), 4.37 (t, 1H, J = 5.7 Hz), 4.75 (s, 1H), 4.89 (s, 1H), 5.40 (d, 1H, J = 8.4 Hz), 6.66 (d, 2H, J = 8.6 Hz), 7.16−7.22 (m, 3H), 7.24−7.27 (m, 2H), 7.40 (s, 1H), 7.51 (d, 2H, J = 8.6 Hz); ^{13}C NMR (125 MHz, $CDCl_3$) δ 23.7, 30.0, 33.9, 35.9, 38.1, 39.5, 41.7, 54.6, 54.8, 55.9, 57.6, 67.7, 74.0, 76.6, 84.0, 114.1, 124.9, 126.2, 128.2, 129.3, 129.4, 137.9, 151.0, 156.2, 178.4. LRMS-ESI (m/z) [M + Na]$^+$ 609.0; HRMS-ESI (m/z) [M + Na]$^+$ calcd for $C_{29}H_{38}N_4NaO_7S$ 609.2359, found 609.2362.

(*R*)-*tert*-Butyl-4-(((2*R*,3*S*)-3-(*tert*-butoxycarbonylamino)-2-hydroxy-4-phenylbutylamino)methyl)-2,2-dimethyloxazolidine-3-carboxylate 22. To a solution of the (*R*)-*tert*-butyl 4-(azidomethyl)-2,2-dimethyloxazolidine-3-carboxylate **21** (411 mg, 1.60 mmol) in MeOH (10 mL) was added Pd/C (40 mg). This mixture was stirred